Chapter 5

Effect of oxalate capped iron oxide nanomaterials

5.1. Introduction

Dietary deficiency of iron afflicts billions of people in the world [1]. Fe is an essential micronutrient element for several agricultural crops. It plays a vital role in chlorophyll synthesis, chloroplast structure and many enzymatic activities (viz. cytochrome in electron transport chain) [2] etc. Plants being the main source of iron in human diet also suffer when the nutrient is deficient in soil. When iron is directly applied to soil, it is easily oxidized or precipitated, and plants cannot utilize this nutrient. Fe deficiency is a global concern for calcareous or alkaline soil due to high pH and low Fe availability [3]. Intensive Fe deficiency shows chlorotic symptom in plant leaves. Fe toxicity problems are prevalent in mainly waterlogged soils. Fe deficiency in soil hinders crop productivity due to formation of insoluble ferric oxides in soil solutions. Soil phosphorus availability is also dependent on their adsorption by iron oxide.

Ferrous sulphate is one of the most commonly used iron salt and widely used in agriculture through foliar spray or soil application [4]. However, prolong use of $FeSO_4$ induce soil acidity; greatly insolubilize bioavailable P ($H_2PO_4^-$ or HPO_4^{2-}) in acid soils. When soil pH is greater than 5.3 the ferrous iron readily oxidizes to plant unavailable ferric form (Fe^{3+}). Hence balancing the Fe and P availability in soil is highly challenging. In this context, efforts have been made in synthesis of Fe based nanoparticles to use as a nanofertilizer in agriculture. He et al. [5] reported the positive effect of iron oxide nanoparticles on C and N cycle in soil. Increased pod and leaf dry weight has been observed in soybean due to application of iron oxide nanoparticles [6]. Moreover, they have been widely applied to decontaminate soils from arsenic [7]. Interestingly, because of their small size, high magnetism, redox states, and agglomeration property, these nanoparticles may provide structural stability to soils in addition to ensuring Fe availability in deficient soils. Although chelated (e.g., EDTA, DTPA etc) Fe fertilizers are used to increase the utilization efficiency, the soil pH often interfere with the stability of chelated compounds [8]. As such, application of Fe nanoparticles can be a useful proposition because these may not acidify the soil in the

same way. However, report of in-depth research in the arena of environmental impacts of nanoparticles is rather scanty in the literature.

Under these perspectives, an efficient, sustainable, cost effective, and green procedure for the large scale synthesis of selective orthorhombic iron(oxalate) capped Fe(0) [Fe(ox)–Fe(0)] nanomaterial was formulated without the use of high temperature calcination. Interestingly, the transformation of Fe(0) to Fe_3O_4 in the synthesized [Fe(ox)–Fe(0)] nanomaterial was observed in water after stirring the reaction mixture at room temperature for 14 h. The oxidized orthorhombic iron oxalate capped Fe_3O_4 nanomaterial [hereafter OCIO] was further characterized by different physical methods such as FTIR, XRD, FESEM, and TEM. Eventually, the synthesized OCIO was applied in an alluvial soil in various concentrations to evaluate the influences on physico-chemical properties of the soil. Quite a few lab scale mimic experiments have been designed and conducted to appreciate the underlying mechanism of the nanoparticles induced changes in soil properties. Moreover, the solubility pattern of major ions in soil samples treated with OCIO were assessed and predicted dissolution/adsorption dynamics through Visual MINTEQ geochemical models. Finally, the significance of the synthesized OCIO in regard to correction of Fe deficiency in soil and thereby the physiological benefit at plant level also been assessed.

5.2. Materials and methods

5.2.1. Synthesis of Oxalate capped iron oxide nanomaterials (OCIO)

In a typical procedure, 34.7 g of $FeSO_4.6H_2O$ and 9.45 g of oxalic acid was added in 400 mL of distilled water to prepare a solution in a 1L beaker and stirred for 20 minutes. Thereafter, a solution of 30 g of $NaBH_4$ was prepared in 100 mL distilled water and added drop wise in the earlier prepared solution under vigorous stirring. During the addition, the color of the solution slowly turns into yellow then green and finally black iron nanomaterials began to appear in the solution. After completion of the reaction, the reaction mixture was kept under stirring at 50° C for 14 h. During this, black colour solution slowly turns into yellow-brown and finally brown color

material was collected in 42 g amount after centrifuging and oven drying at 80°C for 8 hours [9].

5.2.2. Effect of OCIO on beneficial soil bacteria (N-fixing and P-solubilizing) and seed germination indices

The effect of OCIO was assessed on the growth of two beneficial soil bacteria [(N-fixing (NFB) and P solubilizing (PSB)] by following disk diffusion method [10] The efficacy of *Rhizobium sp*. in N-fixation in legume plants and *Serratia marcescens* in P-solubization is well known. These two were selected as the test species. The procedure for determination of antimicrobial activity was described below:

1. Mueller Hinton agar medium was prepared and sterilized in autoclave at 103421.36 Nm^{-2} for 15 minutes before spread plate technique was performed.

2. 100 µL of the bacterial isolates were placed in each petriplate and the cultures were incubated at 28° for 48 hours in BOD incubator.

Additionally, the colony growth of total bacteria was counted in soil treated with OCIO treatments by following pour plate technique [11] as described in Chapter 4 (section 4.2.2.1.5). Nutrient agar medium were used to enumerate the colony count of total bacteria. Each treatment was replicated for three times and the inoculated plates of nutrient agar were incubated at 36°C for 24 hours. Colony forming unit was calculated by the formula mentioned in chapter 4 (section 4.2.2.1.5).

The effect of OCIO on germination of *Vigna radiata* and *V. mungo* seeds was evaluated. 2 mg of OCIO, $FeSO_4$, Fe-EDTA, and Fe-oxalate were dissolved in 10 mL distilled de-ionized water and sonicated for 5-10 minutes. In the meantime, 10 seeds of both the species were placed in glass petri plates containing tissue paper. Then, the previously mentioned treatment solutions were poured in the respective plates and incubated in dark at 25°C for 48 hours. The germination index (GI), relative seed germination (RSG), and relative root growth (RRG) were enumerated by following Karak et al. [12]. The equations for RSG, RRG, and GI have been mentioned in chapter 4 in section.

5.2.3. Effect of oxalate capped iron oxide nanoparticles on earthworm health and proliferation

Eisenia fetida has been duly recognized as a reliable model for soil toxicity assays according to the OECD and EPA guidelines [13]. In this study juvenile, non-clitellated specimens of *E. fetida* (approximately 300-450 mg weight) were used. Then, earthen perforated vessels of 3l capacity were filled with urine free cow dung and the earthworm specimens were inoculated into the substrate @ 10 worm kg^{-1}. This experiment was conducted for 60 days in the late spring. Optimum moisture condition was sustained by sprinkling water at an interval of 2-3 days. Earthworm count and body weight were monitored at 10 days interval, upto 60 days.

Uptake of Fe in earthworm body was analyzed by di-acid digestion method. Well grown and clitellated earthworms were collected from the experimental pots at 60 days. Collected earthworms were properly washed, placed on a moist filter paper and kept overnight for gut cleaning. Afterwards, the gut cleaned earthworms were digested in a di acid mixture [$HClO_4$: HNO_3 (1:6)] solution then diluted with 25 mL of milli-Q water and filtered through Whatmann no 42 filter paper and collected the filtrate. This filtrate was used to analyze the Fe content in UV-VIS Spectrophotometer.

Catalase [14], reduced glutathione (GSH) [15], super oxide dismutase (SOD) [16], lipid peroxidation [17], and total protein content [18] in the OCIO exposed earthworms were determined in both treated and untreated earthworm samples collected after 60 days of inoculation period. The detail protocols for all these attributes except SOD have been furnished in previous sections (chapter 4; sections: 4.2.2.2.5.1, 4.2.2.2.5.2, 4.2.2.1.4.2.2.3 and 4.2.2.2.5.5 respectively). Therefore, here the protocol details for SOD analysis is given below in section 5.2.3.2.

5.2.3.1. Earthworm count and body weight

Earthworm count and body weight was measured manually in a periodical manner starting from 10 days to 60 days.

5.2.3.2. Super oxide dismutase (SOD)

Reagents:

1. 200 mM phosphate buffer (pH 7.6) containing 1mM EDTA
2. 3:5 mixtures of $CHCl_3$: EtOH
3. 15 mM hematoxylin solution prepared in 50 mM phosphate buffer (pH 7.5).

Procedure:

1. 20% tissue homogenate was prepared in 200 mM phosphate buffer (pH 7.6) containing 1mM EDTA.
2. Then, the homogenate was mixed with equal volume of 3:5 mixtures of $CHCl_3$: EtOH and vortexed vigorously and centrifuged at 10,000 g for 15 min.
3. The upper transparent $CHCl_3$ layer containing mostly membrane fractions. Add 10 µL of this upper layer to 990 µL of 15 mM hematoxylin solution prepared in 50 mM phosphate buffer (pH 7.5).
4. The decrease in absorbance was studied for 1 min at 556 nm.

Result:
Results expressed as units SOD/mg protein.

5.2.4. Fe release profile of OCIO in aqueous medium of various pH and the effect on P and N solubility

The efficacy of the synthesized compound (OCIO) on pH variation was determined by introducing it to various ranges of pH solutions (pH 4, 5, 6, 7, 8, and 9). An identical amount (10 mL) of required pH solutions were prepared with an acid (HCl) and a base medium (NH_4OH) correspondingly in Erlenmeyer flasks. A measured amount (0.1 g) of OCIO, Fe-EDTA, $FeSO_4$, and Fe-oxalate was diluted separately in the flasks and kept under continuous shaking in a mechanical shaker for 72 hours @ 120 rpm. Samples were collected periodically at 12, 24, 48, and 72 hours and shift in pH and Fe release was recorded in Eutech pH meter and ICP-OES respectively [19,20].

Common soluble salts of N [$(NH_4)_2SO_4$] and P [KH_2PO_4] were used to analyze the effects of OCIO on P and N solubility in lab scale mechanistic studies. To analyze the effects of OCIO on P solubility, 10 g of OCIO, $FeSO_4$, Fe-EDTA, and Fe-oxalate

were mixed with 10 g of KH_2PO_4 in separate Erlenmeyer flasks and 100 mL of milli Q water were added and placed on a mechanical shaker for continuous shaking at 120 rpm for 21 days. Samples were periodically collected at 24, 48 hours, 7, 14, and 21 days and changes in pH, P, and Fe solubility were recorded by following standard methodologies [19,20]. A similar study was conducted with an easily soluble salt of N [$(NH_4)_2SO_4$] to identify the changes in pH, N, and S solubility in the filtered suspensions. The experimental setup was similar with that of KH_2PO_4. Collection of periodical samples was done at 24, 48 hours, 7, 14, and 21 days and changes in pH, release of N, S, and Fe were determined by following standard methods [19,20].

5.2.4.1. pH

The methodology for pH has been described in chapter 4 (section 4.2.2.2.2.1.1).

5.2.4.2. N availability

The methodology has been described in chapter 4 (section 4.2.2.1.1.4).

5.2.4.3. Phosphate availability

The methodology has been described in chapter 4 (section 4.2.2.2.2.2.3).

5.2.4.4. Fe availability

Aqueous samples were collected and the Fe content was determined in ICP-OES.

5.2.5. Solubility experiment and application of geochemical model Visual MINTEQ

Collected soil samples from the yard study was mixed with distilled deionized water [1:10 (w/v)] in Erlenmeyer flasks. Then, the flasks were fitted on a mechanical shaker fixed at 120 rpm and continuously shaken for 21 days. Samples were collected at 7, 14, and 21 days, filtered through Whatmann no. 1 filter paper. One portion of the filtrate was stored for ICP analysis of cations (2-3 drops of 6N HNO_3 was applied to the filtrate to avoid fungal contamination). The non-acidified samples were undergone for various analyses such as: pH, alkalinity, SO_4^{2-}, PO_4^{3-}, NO_3^-, and Cl^- by following standard methodology [21].

For analysis of various cations, a portion of filtrate from each sample was taken out and acidified with concentrated HNO_3. Then Fe, Mn, Ca, and Mg concentrations were analyzed in UV-Vis spectrophotometer and ICP-OES respectively [20].

5.2.5.1. pH

The methodology has been described in chapter 4 (section 4.2.2.2.2.1.1).

5.2.5.2. Total Alkalinity

Reagents:

1. Phenolphthalein solution: 0.5 g of phenolphthalein was dissolved in 50 mL 95% ethanol solution.
2. Methyl orange indicator: 0.5 g of methyl orange was dissolved in 100 mL distilled water.
3. Standard (0.02 N) Sulphuric acid solution: 1.4 mL of H_2SO_4 (36 N) was taken in a volumetric flask and volume made upto 1 L with distilled water.

Procedure:

1. 5 mL of liquid sample was taken in a 100 mL Erlenmeyer flask and diluted to 25 mL by addition of distilled water.
2. Then, phenolphthalein indicator (2-3 drops) was added into it. Titration with standard H_2SO_4 was skipped in this step because solution colour wasn't changed due to application of phenolphthalein indicator.
3. Again, 5 mL of liquid sample was taken in a 100 mL Erlenmeyer flask and 2-3 drops of methyl orange indicator was added into it. Titration was done with standard H_2SO_4 acid solution. At the end point of titration yellow colour of the solution was turned into rosy red.

Calculation:

$$\text{Carbonate}\left(\frac{\text{ml}}{\text{L}}\right) = \frac{\text{PR} \times 2 \times \text{N} \times 1000}{\text{V}}$$

PR: phenolphthalein reading, N: H_2SO_4 normality, V: aliquot volume.

$$\text{Bicarbonate (ml/L)} = \frac{(\text{MR} - \text{PR}) \times 2 \times \text{N} \times 1000}{\text{V}}$$

MR: Methyl orange reading, PR: phenolphthalein reading.

5.2.5.3. Phosphate

The methodology has been described in chapter 4 (section 4.2.2.2.2.2.3).

5.2.5.4. Sulphate

The methodology has been described in chapter 4 (section 4.2.2.2.2.2.5).

5.2.5.5. Nitrate

The methodology has been described in chapter 4 (section 4.2.2.1.3.2).

5.2.5.6. Chloride

Reagents:

1. K_2CrO_4 indicator: 5g of K_2CrO_4 was dissolved into 75 mL distilled water and $AgNO_3$ solution was added to it in a drop wise manner to form a red precipitate. After that the solution was filtered and the filtrate was diluted to 100 mL with distilled water.
2. Standard $AgNO_3$ solution: 4.791 g of $AgNO_3$ was taken into a 1000 mL volumetric flask and volume was made up with distilled water.
3. Standard NaCl solution: 1.648 g of NaCl was dissolved into 1L distilled water.

Procedure:

Standardization of $AgNO_3$ solution:

1. From NaCl solution 10 mL was taken and the volume was made upto 100 mL with distilled water.
2. Then, 0.5 mL of K_2CrO_4 indicator was added into the solution and titrated with standard $AgNO_3$ solution.
3. At the end point of titration stable red precipitation was formed in the solution.
4. From titration the factor of strength of $AgNO_3$ solution was standardized.

   F=the factor of $AgNO_3$ concentration,

   V=the volume required for titration,

   $$F = \frac{10}{V}$$
5. For sample analysis 20-100 mL of liquid sample was taken in conical flask and titrated with standard $AgNO_3$ solution till appearance of permanent red precipitation.

Calculation:

$$\text{Concentration of Chloride (ppm)} = \frac{X \times F \times 1000}{V}$$

Where, X=titre value (mL), F=Factor, V=aliquot volume (mL)

5.2.5.7. Spectrophotometric determination of Iron concentration

1. Standard iron solution was prepared by dissolving 0.25 g of $FeSO_4$ in 1000 mL distilled water.
2. Then, 25.00 mL of this standard iron solution taken into a 500 mL volumetric flask and dilute up the mark with distilled water.
3. Different concentration of iron solution was prepared by pipetting the indicated amounts of the above iron solution into labeled 50 mL volumetric flasks. A blank was kept containing no iron solution.

Concentration of Fe	Volume to pipet
0.00 mg	0.00 mL
0.05 mg	4.00 mL
0.10 mg	8.00 mL
0.15 mg	12.00 mL
0.20 mg	16.00 mL
0.25 mg	20.00 mL

4. To determine Fe concentration in unknown sample first 10.00 mL of sample solutions were taken into 250 mL volumetric flasks and diluted to the mark with distilled water and mixed well.
5. Then, 25.00 mL aliquots of these solutions were taken into 50 mL volumetric flasks and 4.0 mL of 10% hydroxylamine hydrochloride solution and 4.0 mL of 0.3% o-phenanthroline solution was added to each volumetric flask.
6. The solutions were then allowed to stand for 10 minutes and diluted with distilled water.
7. Each sample (including calibration solutions) was scanned in scan analysis programme in UV-VIS Spectrophotometer within 200-800 nm range.
8. A calibration curve was prepared by plotting the datas of absorbance versus concentration of the known solutions and from this standard curve Fe

concentration was determined. The calibration curve was attached in Annexure.

5.2.5.8. Mn, Ca, and Mg determination

Liquid samples were collected and Mg, Ca, and Zn content were determined in ICP-OES.

5.2.6. Soil conditioning and plant growth promoting potential of OCIO: Pot culture experiments

Two pot culture experiments were designed with a typical alluvial soil type to address the impacts of OCIO on soil quality. The soil was rich in iron and overall nutrient composition (NPK etc.); therefore in one set, all nutrients including iron were artificially leached out till the Fe concentration gone below the detection limit of the ICP-OES.

Collected soil samples were air dried, removed plant parts, and sieved through a 2 mm mesh sieve. Then a glass column (5 cm dia) was uniformly filled with the soil samples and distilled demonized water was passed through it at a uniform flow rate for 96 hours till pH decreases to 6.3 and Fe content to below detection limit. 1 kg of this artificially leached soil samples were filled separately into burnt earthen pots and subsequently inoculated with a uniform dose (50 mg kg^{-1}) of OCIO, $FeSO_4$, Fe-EDTA, Fe-oxalate and one control for basic comparison. Then, nursery raised tomato (cv Badshah *F1 hybrid*) seedlings of 2-3 leaf stages were transplanted in each pot and the whole experiment replicated thrice. F1 tomato hybrid occurs when one variety of tomato is pollinated by the other variety of tomato plant and from the seeds of this cross pollinated tomato F1 tomato plants originate. They are resistant, high yielding, semi-determinate, and vigorous plants. Maturity occurs almost after 60-75 days of transplantation. Average weight of fruit is almost 90-100 g.

The Fe deficiency was monitored on the basis of leaf chlorosis symptoms. The crop was harvested after 60 days; changes in pH, avl P, Fe, and phosphatase activity in soil were analyzed following the methods stated earlier [19,22]. Finally, the chlorophyll content, tomato yield (g per plant), and P and Fe uptake in plants was measured following established methods [21,23].

In another set, the natural properties of the soil were not manipulated. Composite soil samples were collected from a nearby farmer's field of Tezpur University (Napaam, Tezpur, Assam). Then, the collected soil samples were air dried, clods were broken, plant parts mixed were removed and natural condition of the soil was maintained through sieving by a 2 mm mesh sieve. Afterwards the prepared soil samples were filled into earthen vessels of 2 L capacity and treated with different doses of OCIO, $FeSO_4$, Fe-EDTA, and Fe-oxalate with one control as shown below:

Table 5.1: Treatment combinations for pot scale study in Fe rich soil

Control					
$FeSO_{4\ 50}$-	$FeSO_4$ @ 50 mg kg^{-1}				
$OCIO_{10}$ -	Fe-(ox)-Fe_3O_4 @10 mg kg^{-1}	$Fe\text{-}EDTA_{10}$ -	Fe-EDTA @ 10 mg kg^{-1}	$Fe\text{-}oxalate_{10}$ -	Fe-oxalate @ 10 mg kg^{-1}
$OCIO_{20}$ -	Fe-(ox)-Fe_3O_4 @20 mg kg^{-1}	$Fe\text{-}EDTA_{20}$ -	Fe-EDTA @ 20 mg kg^{-1}	$Fe\text{-}oxalate_{20}$ -	Fe-oxalate @ 20 mg kg^{-1}
$OCIO_{50}$ -	Fe-(ox)-Fe_3O_4 @50 mg kg^{-1}	$Fe\text{-}EDTA_{50}$ -	Fe-EDTA @ 50 mg kg^{-1}	$Fe\text{-}oxalate_{50}$ -	Fe-oxalate @ 50 mg kg^{-1}

This study was conducted for 90 days and samples were periodically collected at 0, 45, and 90 days respectively. Physico- chemical attributes of collected soil samples [pH, water holding capacity (WHC), bulk density (BD), soil organic carbon (SOC), available nitrogen (avl N), available phosphorus (avl P), and exchangeable potassium (exch K)] were analyzed by following well established methodology [19,24]. The activity of urease and phosphatase enzymes and microbial biomass carbon (MBC) in the treated soil were analyzed following standard methods [22,25,26]. Fe availability was estimated through DTPA extractable methods in ICP-OES [27].

The impact of OCIO on changes in surface characteristics of the treated soil samples were analyzed through BET (NOVA 1000E) surface area analyzer. However, Dynamic light scattering (DLS) (Microtrac MN 401, USA) measurement was also conducted to assess the changes in agglomeration and dispersion profile of the OCIO

treated soil samples. Preparation of soil samples for DLS study was done by following Das et al. [28].

The majority of the protocols followed in this experiment have already been given in previous sections as shown below:

5.2.6.1. pH

The methodology has been described in chapter 4 (section 4.2.2.1.1.3).

5.2.6.2. Water holding capacity

The methodology has been described in chapter 4 (section 4.2.2.1.1.2).

5.2.6.3. Bulk density

The methodology has been described in chapter 4 (section 4.2.2.1.1.1).

5.2.6.4. Soil organic carbon

The methodology has been described in chapter 4 (section 4.2.2.1.1.7).

5.2.6.5. Available nitrogen

The methodology has been described in chapter 4 (section 4.2.2.1.1.4).

5.2.6.6. Available phosphorus

The methodology has been described in chapter 4 (section 4.2.2.1.1.5).

5.2.6.7. Available potassium

The methodology has been described in chapter 4 (section 4.2.2.1.1.6).

5.2.6.8. Microbial biomass carbon

The methodology has been described in chapter 4 (section 4.2.2.2.1.5).

5.2.6.9. Urease activity

The methodology has been described in chapter 4 (section 4.2.2.1.1.8).

5.2.6.10. Phosphatase activity

The methodology has been described in chapter 4 (section 4.2.2.1.1.9).

5.2.6.11. Fe content

The methodology has been described in chapter 4 (section 4.2.2.2.1.8).

5.2.6.12. Zeta potential & hydrodynamic diameter (HDD)

Determination of zeta potential and hydrodynamic diameter (HDD) was done in DLS instrument. The methodology has been described in chapter 4 (section 4.2.2.2.3).

5.2.7. On-field trial: large scale application

5.2.7.1. Experimental site and soil quality analyses

This experiment was conducted in a nearby agricultural field of Tezpur University campus. Field scale experimentation of OCIO was conducted at the same time period as mentioned for field study of AgNP. The average daily temperature range was 17° to 30°C and humidity recorded was 72 to 85% during the experimental period (June 2015 to April 2017).The soil of the experimental field was alluvial (typic endoaquept), sandy loam in nature, and acidic in reaction. For basic characterization, initially composite soil samples (0-30 cm) were collected from various point of the experimental field before transplantation of seedlings and various physico-chemical attributes (pH, avl N, avl P, exch K, and soil organic carbon) and activities of vital soil enzymes (urease and phosphatase activities) were determined following standardized methods [19,22,25]. The microbial biomass carbon & nitrogen (MBC and MBN) content in soil samples were analyzed by following Vance et al. [26]. Fe content was determined through DTPA extraction method [27].

5.2.7.2. Design of experiment

The experiment was conducted with 4 different concentrations (2, 5, 10, and 20 kg ha^{-1}) of OCIO and Fe-EDTA with $FeSO_4$ (20 kg ha^{-1}) as positive control. Tomato (Badshah *F1 hybrid*) was selected as the test crop for this study. Total 40 plots (6 sq m each) were prepared to allocate all the treatments and control by following complete randomization block design (RBD) method with four replicates for each treatment combinations and control. Four numbers of replicates were selected for each treatment

combinations. As per horticultural practices crop trial should have usually 3-6 replications and with more replications more statistically significant results can be measured. However, with the larger number of replications the cost and time consumption of the experiment will have also increase. For statistical analysis also three numbers of replications is sufficient. So, considering all these factors, four replications were taken for each treatment combinations. This study was conducted consecutively for two years (2015-2016 and 2016-2017).

5.2.7.3. Nursery land preparation and plot size

A field nursery land was prepared to sustain the initial growth of the tomato seedlings. Concurrently, the experimental plot preparation also conducted through ploughing the field of sized 2 m height and 3 m width. Almost after one month of nursery bed preparation the tomato seedlings of 2-3 leaf state were transplanted to experimental plots and further the experiment was carried out.

5.2.7.4. Treatment combinations

The field experiment was conducted with the following treatments for two years with tomato as test crop:

a. OCIO: 2, 5, 10, and 20 kg ha^{-1}

b. Fe-EDTA: 2, 5, 10, and 20 kg ha^{-1}

c. $FeSO_4$: 20 kg ha^{-1}

d. Control

The recommended dose of NPK for tomato (N: 75 kg ha^{-1}, P_2O_5:60 kg ha^{-1}, K_2O: 60 kg ha^{-1}) were applied in each treated plot and control.

5.2.7.5. Agronomic practices

The detailed agronomic practices are presented in a table in Annexure.

5.2.7.6. Periodical sampling & physico-chemical assessment of the plant and soil samples

Soil samples collected from different points of the experimental plots were mixed properly to prepare composite samples for each replicates after air drying, breaking the clods, removing plant parts, and sieving through 2 mm mesh sieve. Then, the prepared samples were stored in plastic sample containers in ambient temperature condition with proper labeling and undergone analysis of all the soil quality attributes mentioned.

To assess the effect of nanoparticles on crop performance observations was taken periodically on crop growth and the yield attributes, Shelf life, Chlorophyll and carotenoid content [23], lycopene content [29], tomato yield, nutrient (N, P, and Fe) uptake [21].

5.2.7.7. Effect of OCIO on crop growth, photosynthesis, hill activity, oxidative stress, and expressions of vital enzymes and their genes

Ripened tomatoes were harvested from the field and yield was assessed. However, plant samples were also collected between 35-45 days after transplanting (grand growth stage) from selected plots for enzyme assays and molecular assessments. For the purpose of the study, the plants grown in plots treated with lowest dose (2 kg ha^{-1}) of OCIO were selected and compared with $FeSO_4$ (20 kg ha^{-1}) and Fe-EDTA (10 kg ha^{-1}) treated plants to avoid gross removal of plant biomass before maturation. Chlorophyll content and hill activity were analyzed by following standard methodologies discussed earlier in detail in chapter 4, sections 4.2.2.1.4.1.6 and 4.2.2.1.4.2.1.6 [23,30]. Photosynthetic rate was enumerated in LICOR 6400 photosynthetic meter.

The impacts of OCIO on activities of some vital enzymes and their genes related to N-assimilation and amino acid synthesis were also enumerated in this study by estimation of glutamine synthetase (GS) [31], glutamate synthase (GOGAT) [32], nitrate reductase (NR) [33] activity and expression of their respective gene (*GS*, *GOGAT*, and *NR*) in qRT-PCR method by following standard methodologies [28].

Moreover, the expression of *Fd* gene was determined to identify the effect of OCIO on photosynthesis of plants.

5.2.7.7.1. Glutamine synthetase (GS)

The methodology has been described in chapter 4 (section 4.2.2.1.4.2.3.2).

5.2.7.7.2. Glutamate synthase (GOGAT)

The methodology has been described in chapter 4 (section 4.2.2.1.4.2.3.3).

5.2.7.7.3. Nitrate reductase

The methodology has been described in chapter 4 (section 4.2.2.1.4.1.9).

5.2.7.7.4. Gene expression in qRT-PCR

The methodology has been described in chapter 4 (section 4.2.2.1.4.1.10).

5.2.7.8. Assessment of oxidative stress in OCIO treated plants

Determination of catalase [34], lipid peroxidation [17], and super oxide dismutase [17] were performed to assess oxidative stress induced in plants under various treatments.

5.2.7.8.1. Catalase activity

The methodology has been described in chapter 4 (section 4.2.2.1.4.2.2.1).

5.2.7.8.2. Lipid peroxidation

The methodology has been described in chapter 4 (section 4.2.2.1.4.2.2.3).

5.2.7.8.3. Super oxide dismutase

Superoxide dismutase activity was estimated by recording its ability to inhibit photochemical reduction of nitroblue tetrazolium (NBT).

Reagents:

1. 1.5 M Na_2CO_3
2. 200 mM methionine
3. 3 mM EDTA
4. 2.25 mM NBT
5. 100 mM potassium phosphate buffer(pH 7.5)
6. 60 µM riboflavin

Procedure:

1. Initially, 3 mL of a reaction mixture was used containing 0.1 mL of 1.5 M Na_2CO_3, 0.2 mL of 200 mM methionine, 0.1 mL 3 mM EDTA, 0.1 mL of 2.25 mM NBT, 1.5 mL of 100 mM potassium phosphate buffer (pH 7.5), 0.8 mL of distilled water and 0.1 mL of the enzyme extract.
2. The tube without enzyme was taken as control.
3. The reaction was started by adding 0.1 mL of 60 µM riboflavin and placing the tubes below a light source of two 15 W fluorescent lamps for 15 minutes.
4. The reaction was stopped by switching off the light and covering the tubes with black cloth.
5. Absorbance was recorded at 560 nm in spectrophotometer (UV-1700 series, Pharma spec Japan).

Calculation:

$$\text{SOD} = \frac{\%\text{ reduction in colour between blank and sample } \times \text{Dilution factor} \times 60}{50 \times \text{incubation time} \times \text{mg protein in sample}}$$

$$\text{Where, \% reduction } = \frac{\text{Optical density in light} - \text{Optical density in dark}}{\text{Optical density in light} \times 100}$$

$$\text{Dilution Factor } = \frac{\text{Biomass taken (mg)}}{\text{Volume of extraction buffer}}$$

5.3. Statistical analysis:

One-way and two-way analysis of variance (ANOVA) was performed for eco-toxicity and soil quality experiments respectively. The least significance test (LSD) was also carried out to detect the relative efficiency between different treatments.

5.4. Results:

5.4.1. Characterization and large scale applicability of the synthesized nanomaterial

5.4.1.1. Powder XRD and FT-IR analysis

The synthetic route involved step-wise generation of 3 materials viz. Fe(ox)–Fe(0), $Fe(C_2O_4)\cdot 2H_2O$, and finally the Fe(ox)–Fe_3O_4 or OCIO. The FTIR spectrum of all these 3 materials were recorded and plotted in Fig. 5.1a. The carboxylate coordination mode can be determined from the corresponding position and separation of ν(COO-) bands, Δ, in the 1300–1700 cm^{-1} region. Generally for $\Delta > 200$ cm^{-1}, a unidentate ligand is expected, whereas for $\Delta < 110$ cm^{-1}, it is a bidentate ligand and for a bridging ligand, Δ remains in between. The FTIR spectra of $Fe(C_2O_4)\cdot 2H_2O$ showed peaks at 1640 and 1362 cm^{-1} for typical metal carboxylate, in which oxalic acid is acting as a bidentate ligand. The other two peaks at 1320 and 820 cm^{-1} were due to the C–O and C–C stretching vibration of coordinated oxalic acid in $Fe(C_2O_4)\cdot 2H_2O$. The comparative FTIR spectra of synthesized [Fe(ox)–Fe(0)] and $Fe(C_2O_4)\cdot 2H_2O$ clearly showed the occurrence of iron oxalate in synthesized [Fe(ox)–Fe(0)] as both spectra clearly matched with each other. In contrast, the FTIR spectrum of OCIO [Fe(ox)–Fe_3O_4] nanomaterial showed peaks at 1412 and 1655 cm^{-1} due to the oxalate coordination to metal oxide and two other peaks at 415 and 563 cm^{-1} were due to Fe–O symmetric bending vibration and Fe–O–Fe stretching. However, [Fe(ox)–Fe(0)] material was competent in the reduction of methylene blue to its corresponding leuco methylene blue [35] and on completion of the reaction the black material transformed into brown because of the oxidation of corresponding Fe(0) into its oxide (i.e., Fe_3O_4) (Fig. 5.1b).

The XRD spectrum of all the three materials is presented in Fig 5.1c-d. The spectra of [Fe(ox)–Fe(0)] approved the orthorhombic structure of the $Fe(C_2O_4)\cdot 2H_2O$. However, the presence of Fe(0) in the synthesized material could not be detected from the XRD spectrum as the peaks for Fe(ox) and Fe(0) was overlapping each other. The XRD spectrum of synthesized Fe(ox)–Fe(0) confirmed the presence of orthorhombic, as the peaks in XRD were in good agreement with the reported XRD pattern of $Fe(C_2O_4)\cdot 2H_2O$ (Fig. 5.1c) [36,37]. Correspondingly, the structure of the oxidized (OCIO) material was appeared to be a mixture of typical orthorhombic iron oxalate and magnetite Fe_3O_4 because the peak position and intensity were vividly indicating

their (orthorhombic $Fe(C_2O_4)\cdot 2H_2O$ and Fe_3O_4) occurrence (JCPDS card 85-1436) (Fig. 5.1d) [38].

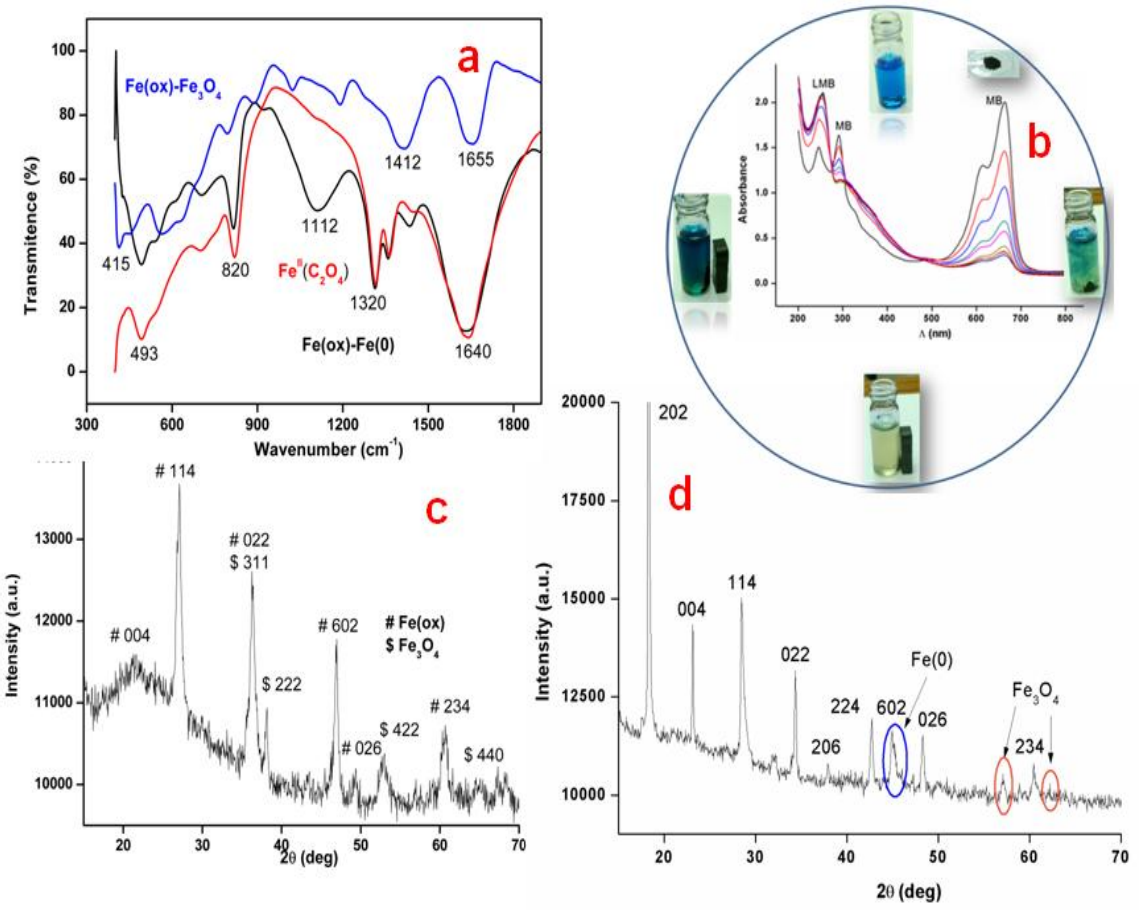

Fig. 5.1: Comparative FT-IR spectrum of Fe(ox)-Fe(0) and Fe(ox)-Fe_3O_4 (OCIO) with Iron oxalate complex (a); Fe(ox)-Fe(0) promoted reversible methylene blue to Leuco methylene blue redox reaction (b); XRD spectrum of Fe(ox)-Fe(0) (c) and OCIO (d), source: Das et al. [9]

5.4.1.2. Morphology, surface and elemental analysis of the synthesized nanomaterial

The surface morphology of the synthesized nanomaterial was analyzed through HR-SEM (Fig. 5.2a). The porous morphology of the OCIO was confirmed by the HR-SEM image. In addition, the EDS analysis of the selected region of the OCIO nanomaterial confirmed the presence of carbon, oxygen, and iron in 17.5, 56.1, and 26.4% respectively (Fig. 5.2b). We were also interested to identify the Fe content in the OCIO. The result showed 28.6 wt% of iron content in the material. Moreover, the surface characteristic of the synthesized OCIO was analyzed through the nitrogen adsorption–desorption isotherm and the pore size distribution of the synthesized

material (Table 5.2). We recorded 55.2 m^2 g^{-1} surface area of OCIO and observed porous nature of the nanomaterial from BET analysis (Fig. 5.3), which was consistent with the morphology revealed from HR-SEM and HR-TEM images (Fig. 5.2c). Interestingly, the HR-TEM images (Fig. 5.2c and d) explained that the synthesized OCIO had ribbon like structure with a size range of 10–100 nm in length and 1–5 nm in breadth. Moreover, the SAED pattern confirmed the 111 and 200 planes of the Fe_3O_4 (Fig. 5.2d). Furthermore, the particle size distribution analysis confirmed that the majority of the particles in the OCIO materials were within the range of 2–5 nm (Fig. 5.2e).

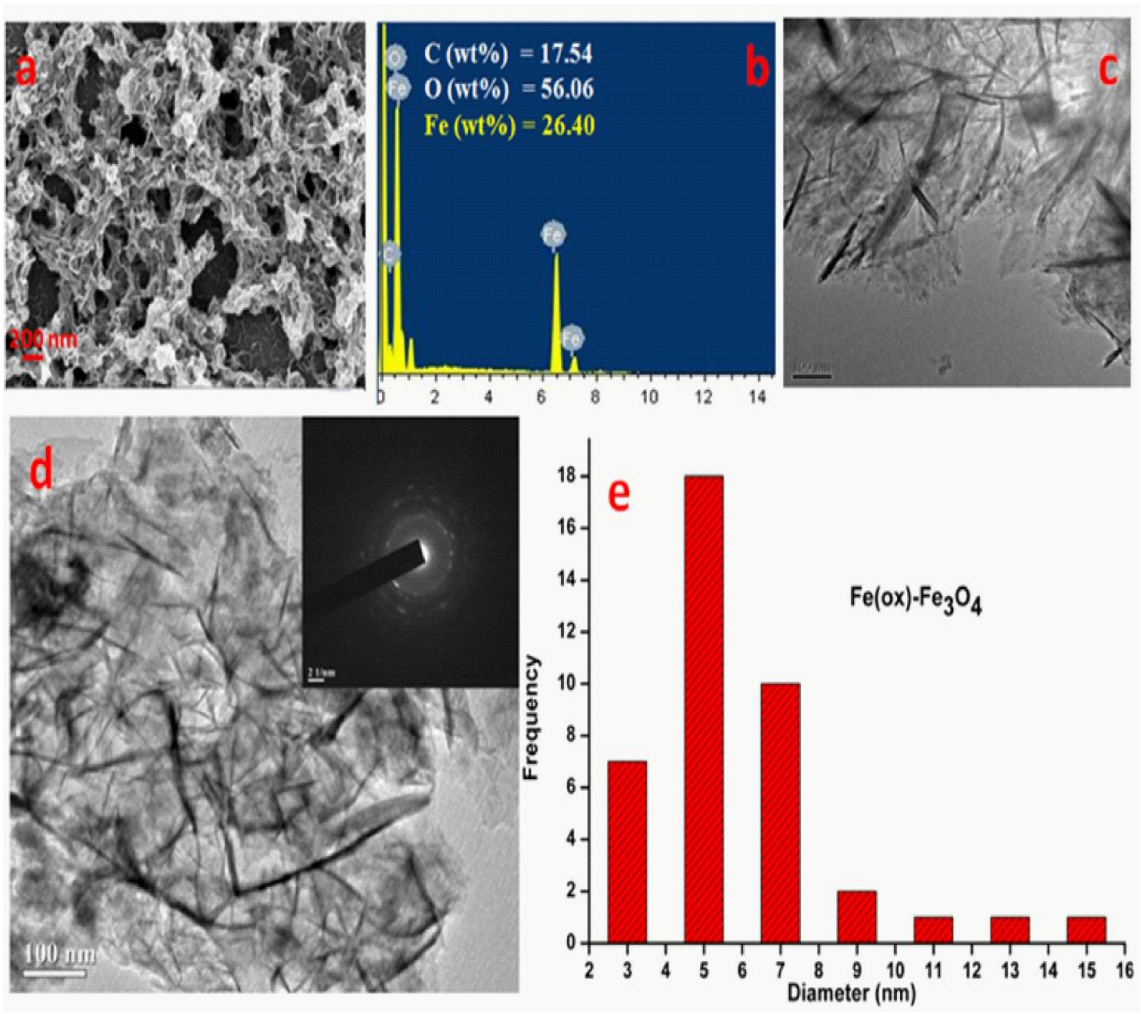

Fig. 5.2: HR-SEM image (a); EDAX (b); HR-TEM image (c); HR-TEM image and SAED (d); and particle distribution analysis (e) of OCIO nanomaterial, source: Das et al. [9]

Table 5.2: Surface area, pore radius, pore volume, and band gap of OCIO, source: Das et al. [9]

Parameters	OCIO
Surface area (m^2g^{-1})	55.2
Pore Radius (Å)	18.332
Pore Volume (ccg^{-1})	0.071
Band gap (eV)	2.0

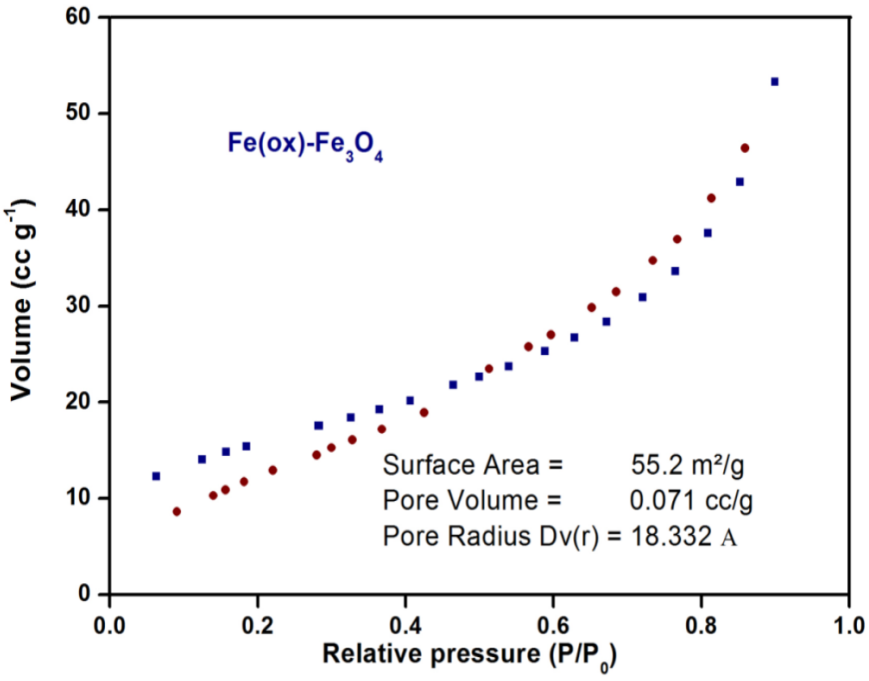

Fig. 5.3: BET plot for OCIO, source: Das et al. [9]

5.4.1.3. Oxidation states of iron: X-ray photoelectron spectral analysis

The valance of iron was important to interpret the changes in soil properties. Hence, X-ray photoelectron spectrometry (XPS) was carried out to analyze the chemical composition and status of Fe–C–O in the OCIO. The XPS (ESCALAB 220i) measurement was performed on the sample with Al α X-ray source; the energy calibration was made against the C 1s peak. As shown in Fig. 5.4a, the XPS scan spectra of Fe–C–O exhibits distinct C_{1s} and O_{1s} peaks at 283.77 eV and 531.9 eV respectively, which confirms the presence of oxalic acid in the synthesized

nanomaterial. It has been previously reported that $Fe_{2p3/2}$ for Fe_3O_4 does not have a satellite peak, which was also confirmed (Fig. 5.4b). The peak positions of $Fe_{2p3/2}$ and $Fe_{2p1/2}$ are 710.86 eV and 724.74 eV respectively clearly match for Fe_3O_4. Another peak was observed at 56.1 eV for Fe_{3p}. The $Fe_{2p3/2}$ peak for Fe_3O_4 was deconvoluted into Fe^{2+} and Fe^{3+} peaks. It is known that stoichiometric Fe_3O_4 can be expressed to $FeOFe_2O_3$, the ratio of Fe^{2+}: Fe^{3+} should be 1 : 2. In our case, the results of the deconvoluted peaks give Fe^{2+}: Fe^{3+} =0.31: 0.69 [39,40] This value satisfies the stoichiometric values with a negligible analytical error (SD=0.1)

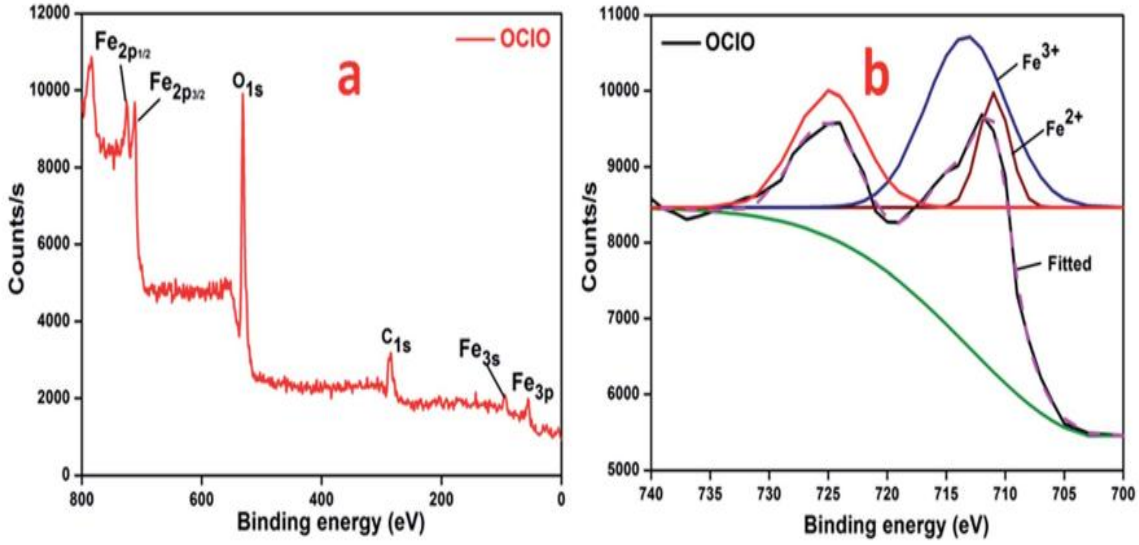

Fig 5.4: Full scan XPS spectra for OCIO (a) and XPS spectra of deconvoluted $Fe_3p_{1/2}$ and $Fe_3p_{3/2}$ (b), source: Das et al. [9]

5.4.2. Effect on soil beneficial bacterial diversity

The data on effects of OCIO on total bacterial growth along with responses of nitrogen fixing bacteria and phosphate solubilizing bacteria to OCIO exposure are presented in Table 5.3, Fig. 5.5a and b respectively. Significantly high bacteria count was recorded in OCIO treated soil as compared to the control (Table 5.3) (P=0.002). This may be due to a steady Fe sustenance contributed by the OCIO material. In addition, antagonistic effect on two well characterized beneficial soil microorganisms (*Rhizobium sp*. and *Serratia marcescens*) was tested. Fascinatingly, no zone of inhibition was noticed even after 72 hours of incubation in the medium. This result ensured the eco-friendly nature of the synthesized OCIO. In addition, the plate count

of colony forming units of both NFBs and PSBs was highly encouraging in OCIO treated soil.

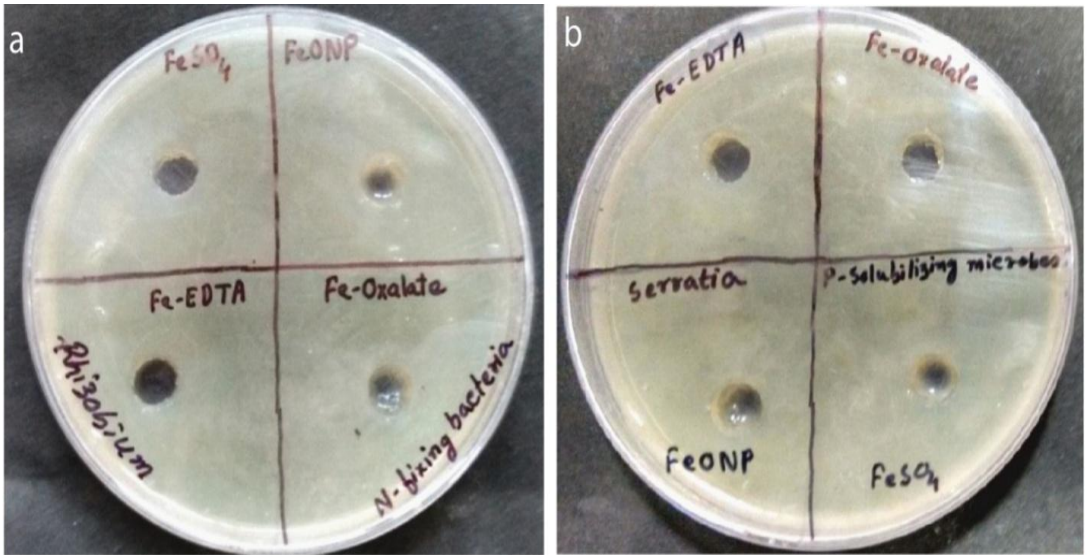

Fig. 5.5: Anti-bacterial assay of the synthesized compound on N-fixing (*Rhizobium sp.*) (a) and P-solubilizing (*Serratia marcescens*) (b) soil bacteria, *FeONP=OCIO, source: Das et al. [9]

Table 5.3: Total bacterial count in soil treated with OCIO, source: Das et al. [9]

Treatments	Colony forming unit $mL^{-1}(\times 10^6)$	
	Initial	90 days
Control	0.1±0.08	0.8±0.06
OCIO	0.4±0.06	2.8±0.1
P value	0.002	
LSD	0.29	

5.4.3. Phytotoxicity: Effect on seed germination assay

Fig. 5.6a and b represent data on the effect of OCIO contributed Fe on seed germination of two pulse crops. Significantly high germination index (GI) was recorded in OCIO treated seeds of *Vigna radiata* and *V. mungo* as compared to the other sources of Fe ($FeSO_4$, Fe–oxalate, and Fe–EDTA) (LSD= 1.33; 1.26) (Fig. 5.6a and b). Concurrently, RSG and RRG were substantially higher in OCIO treated seeds than Fe–EDTA and $FeSO_4$ (LSD: RSG =0.82; RRG=0.93) (Fig. 5.6b).

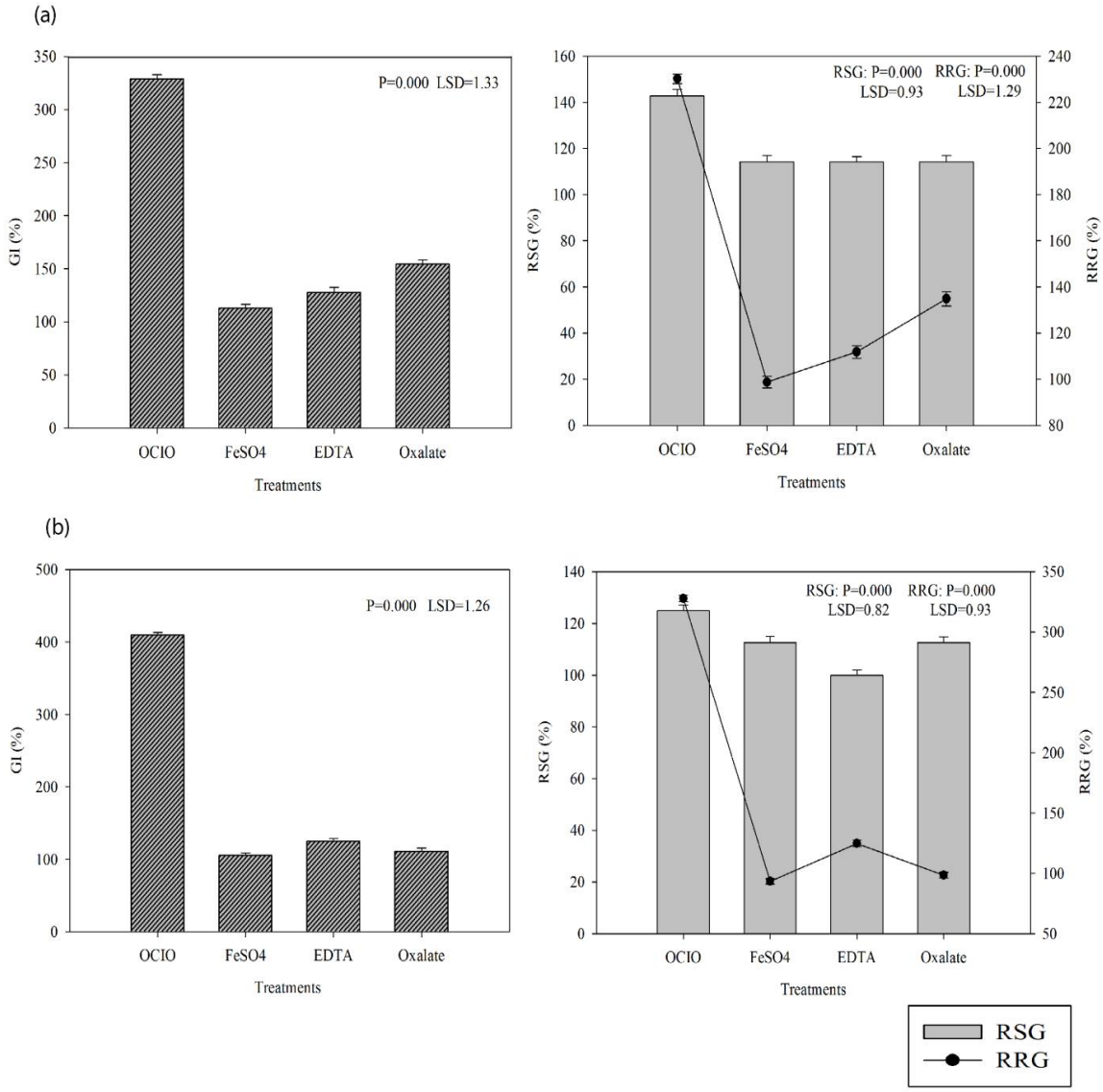

Fig. 5.6: Relative seed germination (RSG), relative root growth (RRG), and germination index (GI) of *V. radiata* (a) and *V. mungo* (b) seeds treated with OCIO, $FeSO_4$, Fe–EDTA and Fe–oxalate, source: Das et al. [9]

5.4.4. Impacts of OCIO on earthworm health and proliferation:

5.4.4.1. Earthworm count and body weight:

Table 5.4 presents the data on earthworm fecundity (count and body weight) in response to OCIO exposure. The density of earthworms significantly increased over time due to OCIO 10 mg kg^{-1} exposure followed by OCIO 20 mg kg^{-1} and OCIO 50 mg kg^{-1}.Whereras, in case of $FeSO_4$ earthworm count decreases after 40 days. At the end of 60 days the number of specimens under various treatments was in the order:

OCIO10 mg kg^{-1}> OCIO 20 mg kg^{-1}>OCIO 50 mg kg^{-1}>Control>$FeSO_4$ 50 mg kg^{-1} (P<0.01; LSD =2.48). On the other hand, the mean bodyweight of *Eisenia fetida* was significantly greater under OCIO 10 mg kg^{-1} exposure as compared to all other treatments.

Table 5.4: Changes in body weight and count of *Eisenia fetida* under OCIO exposure (mean± standard deviation)

		Duration of the experiment					
	Treatment	**10 Day**	**20 Day**	**30 Day**	**40 Day**	**50 Day**	**60 Day**
Body weight	OCIO 10	0.68±0.02	0.79±0.04	0.95±0.05	1.11±0.06	1.39±0.09	1.54±0.11
	OCIO 20	0.71±0.04	0.72±0.04	0.89±0.05	0.94±0.06	1.28±0.1	1.37±0.1
	OCIO 50	0.67±0.02	0.7±0.03	0.79±0.04	0.87±0.07	1.18±0.1	1.24±0.12
	$FeSO_4$	0.56±0.05	0.60±0.03	0.63±0.04	0.70±0.05	0.82±0.07	0.85±0.12
	Control	0.62±0.02	0.64±0.04	0.69±0.05	0.72±0.05	0.87±0.1	0.98±0.11
Count	OCIO 10	19±2.6	28±2	36±2.1	45±2.6	52±2.5	68±3
	OCIO 20	19±1.7	26±2	33±1.5	38±2	46±2.6	55±2.6
	OCIO 50	18±2	23±2.6	31±1.4	33±2	37±2.6	42±2.6
	$FeSO_4$	14±1.7	19±2	20±1.2	24±2.6	22±2.6	21±2.6
	Control	15±1.7	18±2	20±1.1	24±2.6	29±3	32±3.4
P	Body	<0.01	<0.01	<0.01	<0.01	<0.01	<0.01
L.S.D	weight	0.025	0.027	0.03	0.026	0.027	0.034
P		ns	<0.01	<0.01	<0.01	<0.01	<0.01
L.S.D	Count	1.63	1.75	1.96	2.16	2.13	2.48

5.4.4.2. Oxidative stress, total protein, and Fe accumulation in earthworms:

Catalase activity was significantly higher in $FeSO_4$ exposed earthworms (50 mg kg^{-1}) as compared to OCIO (Table 5.5). Correspondingly, GSH and SOD activities were also significantly elevated in $FeSO_4$ exposed earthworms. The SOD activity was 2.85 and 2.25 folds lesser in OCIO 10 and 50 mg kg^{-1} treated earthworms respectively as compared to 50 mg kg^{-1} exposure of $FeSO_4$. Lipid peroxidation was expressed as malondehyde production. Lowest production of malondehyde was recorded in OCIO (10 mg kg^{-1}) treated earthworms. At the end, lipid peroxidation was in the order: $FeSO_4$ 50> Control> $OCIO_{50}$>$OCIO_{10}$ (P<0.01, LSD=1.58) (Table 5.5).

The data on Fe accumulation and protein levels in the earthworms are presented in Table 5.6. Although Fe accumulation was highest in $FeSO_4$ treated earthworms, the total protein content was significantly greater in OCIO 10 mg kg^{-1} exposed

earthworms (P<0.01; LSD=0.013). Hence, the greater accumulation of Fe in $FeSO_4$ treated earthworms could be attributed to the higher dose exposure (50 mg kg^{-1}) than OCIO.

Table 5.5: Activity of catalase, reduced glutathione (GSH), super oxide dismutase (SOD), and lipid peroxidation content in earthworms exposed to OCIO

Treatments	Catalase (mg^{-1} min^{-1})	Reduced glutathione (GSH) (nM mg^{-1})	Superoxide dismutase (SOD) (mg^{-1} min^{-1})	Lipid peroxidation (µM g^{-1})
	Mean±stdev	Mean±stdev	Mean±stdev	Mean±stdev
OCIO10	35.74±1.62	25.66±1.5	49.15±2.6	18.06±1.1
OCIO50	80.11±3.85	48.69±2.5	62.39±4.6	26.67±3.5
$FeSO_4$ 50	315.99±17	81.85±4.1	140.39±7.2	68.17±2.5
Control	172.43±9.5	68.43±3.5	101.36±8.1	52.79±3.2
P value	<0.01	<0.01	<0.01	<0.01
LSD	1.23	0.6	1.66	1.58

Table 5.6: Effect on Fe uptake and total protein content of *E. fetida* treated with OCIO

Treatments	Protein (ug uL^{-1})	Fe uptake (mg kg^{-1})
	Mean±stdev	Mean±stdev
OCIO 10	0.25±0.001	5.6±0.8
OCIO 50	0.23±0.001	15.8±1
$FeSO_4$ 50	0.18±0.002	18±1.1
Control	0.17±0.002	2.9±1
P value	<0.01	<0.01
LSD	0.013	0.129

5.4.5. Influence of the OCIO on pH and Fe release: unique buffering capacity

It was important to validate the relationship of pH and Fe release from OCIO through a simple lab-scale experiment with aqueous solutions of different pH (Table 5.7 and Fig. 5.7a–c). Aqueous solutions of three different pH values (pH: 4, 7, and 9) were treated with OCIO, Fe-EDTA, $Fe(C_2O_4)$, and $FeSO_4$ to appreciate the relationship between pH and release profile of iron. In acidic solutions (pH 4 and 5), the pH significantly shifted towards neutral value (pH – 4 to 6.54; pH – 5 to 6.6) due to OCIO addition; whereas the pH of both the neutral and alkaline solutions increased marginally (pH – 7 to 7.17, pH – 8 to 8.13; pH – 9 to 8.6) over 72 hours (Table 5.7 and Fig. 5.7a). However, sharp acidification was noted in Fe-EDTAs and sulphates treated solutions of all pH. Although Fe release was highest in $FeSO_4$ treated solutions followed by OCIO in acid (pH 4 & 5) solutions; the release was significantly greater in neutral and alkaline solutions due to OCIO addition (pH 7: 28.6±0.24 ppm; pH 9: 17.8±0.18 ppm) (Table 5.7 and Fig. 5.7b).

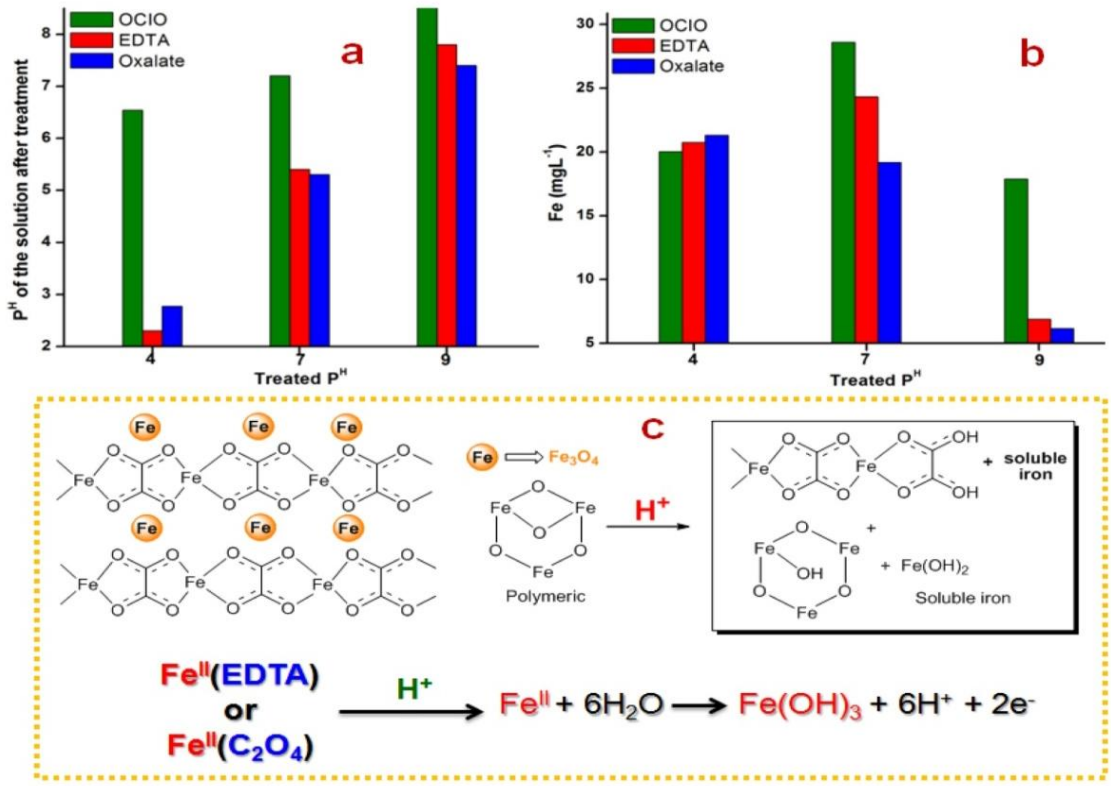

Fig. 5.7: Effect on pH shift (a) and Fe release (b) from OCIO, Fe-EDTA and Fe-oxalate; The proposed mechanism of H^+ ion scavenging property of OCIO (c), source: Das et al. [9]

Table 5.7: Effect of synthesized materials in pH change and Fe content (mg L^{-1}) release, source: Das et al. [9]

	pH change				Fe release (mg L^{-1})			
pH range	**12 h**	**24 h**	**48 h**	**72 h**	**12 h**	**24 h**	**48 h**	**72 h**
OCIO pH 4	6.48±0.05	6.5±0.03	6.53±0.04	6.54±0.2	8.58±0.1	10.73±0.3	15.74±0.1	20.03±0.24
OCIO pH 5	6.52±0.08	6.55±0.04	6.57±0.05	6.6±0.04	10.01±0.2	12.88±0.2	18.5±0.2	22.89±0.3
OCIO pH 6	6.53±0.09	6.56±0.05	6.59±0.04	6.63±0.01	12.88±0.3	15.74±0.3	17.8±0.3	22.89±0.3
OCIO pH 7	7.11±0.05	7.12±0.04	7.15±0.03	7.17±0.1	11.44±0.2	24.3±0.3	25.7±0.3	28.6±0.24
OCIO pH 8	8.13±0.07	8.15±0.03	8.12±0.02	8.13±0.04	15.74±0.3	17.8±0.1	15.74±0.3	17.8±0.2
OCIO pH 9	8.58±0.11	8.58±0.02	8.59±0.02	8.6±0.09	10.73±0.3	15.74±0.2	16.4±0.4	17.8±0.18
Fe-EDTA pH 4	2.34±0.02	2.32±0.01	2.32±0.04	2.3±0.04	10.74±0.3	15.17±0.2	17.03±0.4	20.74±0.26
Fe-EDTA pH 5	2.36±0.05	2.34±0.01	2.33±0.01	2.33±0.02	9.31±0.1	16.6±0.2	19.3±0.4	22.17±0.3
Fe-EDTA pH 6	3.48±0.05	3.44±0.05	3.43±0.01	3.42±0.02	12.04±0.2	15.15±0.2	18.3±0.3	24.33±0.2
Fe-EDTA pH 7	5.46±0.04	5.46±0.01	5.45±0.01	5.44±0.01	17.18±0.3	19.02±0.3	21.17±0.3	24.3±0.22
Fe-EDTA pH 8	6.56±0.03	6.53±0.01	6.5±0.01	6.49±0.02	8.47±0.1	7.89±0.1	5.75±0.1	4.6±0.1
Fe-EDTA pH 9	7.9±0.03	7.89±0.02	7.82±0.05	7.81±0.05	7.31±0.3	7.89±0.2	5.46±0.1	6.89±0.1
Fe-Oxalate pH 4	2.83±0.04	2.8±0.03	2.78±0.04	2.77±0.02	17.17±0.1	18.89±0.4	20.18±0.3	21.33±0.1
Fe-Oxalate pH 5	3.24±0.02	3.2±0.06	3.18±0.05	3.18±0.02	19.31±0.4	23.61±0.4	22.3±0.4	20.03±0.2
Fe-Oxalate pH 6	3.46±0.05	3.45±0.05	3.43±0.05	3.42±0.01	15.04±0.2	26.47±0.4	20.17±0.4	19.2±0.3
Fe-Oxalate pH 7	5.31±0.02	5.3±0.05	5.28±0.05	5.26±0.02	12.89±0.2	26.47±0.3	21.04±0.3	19.17±0.27
Fe-Oxalate pH 8	6.52±0.05	6.51±0.05	6.51±0.06	6.5±0.05	9.45±0.2	9.03±0.3	8.89±0.3	7.44±0.2
Fe-Oxalate pH 9	7.48±0.08	7.47±0.05	7.45±0.08	7.43±0.05	9.29±0.2	8.76±0.3	7.37±0.2	6.16±0.17
$FeSO_4$ pH 4	4.3±0.02	4.4±0.02	4.3±0.02	4.1±0.3	16.12±0.1	18.27±0.4	20.05±0.3	22.1±0.2
$FeSO_4$ pH 5	4.8±0.02	5±0.04	5.1±0.03	4.7±0.05	19.56±0.2	20.79±0.4	22.34±0.2	25.1±0.3
$FeSO_4$ pH 6	5.2±0.02	5.2±0.02	5.4±0.02	5.1±0.03	15.45±0.3	16.35±0.2	15.06±0.1	26.4±0.3
$FeSO_4$ pH 7	5±0.03	5.2±0.02	5.5±0.02	5.4±0.09	11.45±0.3	13.72±0.2	12.06±0.3	25.1±0.3
$FeSO_4$ pH 8	4.8±0.02	5.2±0.02	5.4±0.02	5.4±0.06	10.22±0.2	14.29±0.3	12.56±0.4	10.9±0.1
$FeSO_4$ pH 9	5.5±0.02	5.2±0.02	5.2±0.02	7.21±0.09	10.25±0.3	13.4±0.1	10.63±0.3	5.4±0.1
P value	0.000	0.000	0.000	0.000	0.000	0.000	0.000	0.000
LSD	0.06	0.03	0.02	0.02	0.14	0.17	0.15	0.20

5.4.6. P, N, and Fe release and their interaction in aqueous medium:

A small lab scale experiment was conducted to investigate the underlying mechanisms of high P availability in presence of OCIO (Fig. 5.8). Phosphate ($H_2PO_4^-$) release from KH_2PO_4 significantly enhanced in presence of OCIO in aqueous media ($P<0.01$; $LSD_{treatment}=0.06$) but sharply reduced in presence of ferrous sulphate and Fe-EDTA (Fig. 5.8). While in KH_2PO_4 solutions the release of Fe was significantly greater in presence of OCIO than Fe-EDTA-KH_2PO_4 solutions. In fact, the Fe availability dramatically increased from 69.4 mg L^{-1} to 268.5 mg L^{-1} after 21 days in the OCIO containing solution.

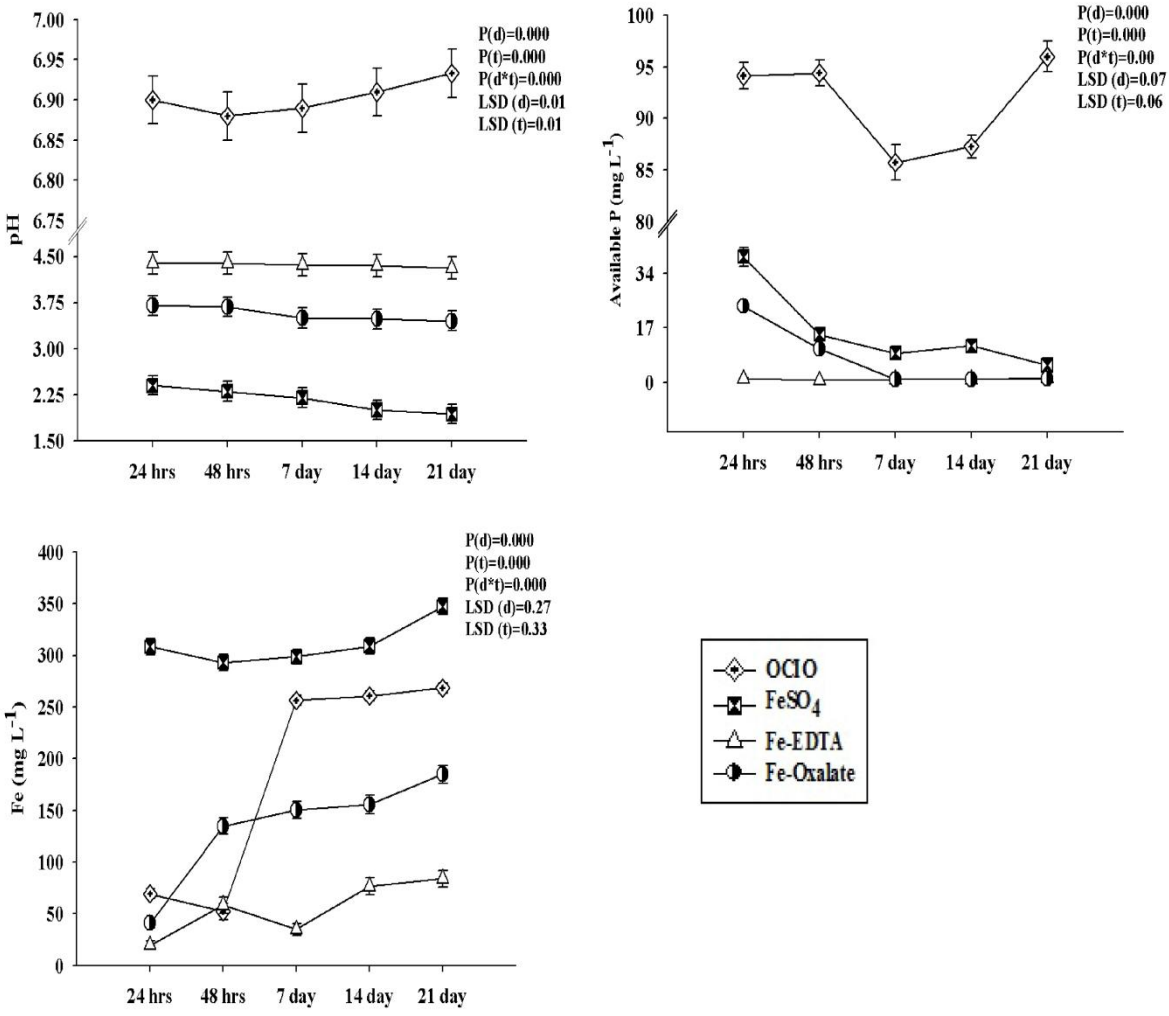

Fig. 5.8: Differences in phosphorous solubility profile from KH_2PO_4 and its interaction with Fe release from OCIO, $FeSO_4$, Fe-EDTA, and Fe-oxalate (*d=day, *t=treatment), source: Das et al. [9]

However, the pH of the $(NH_4)_2SO_4$ mixed solution sharply increased within 24 hours; probably due to NH_3 release, which remarkably neutralized in presence of

OCIO (Table 5.8). Interestingly, the release patterns of Fe and easily mineralizable-N in such solution was in the order: OCIO> $FeSO_4$> Fe-EDTA> Fe-Oxalate ($P<0.01$; N: LSD(trt)= 1.11, Fe: LSD(trt)=0.42), signified the unique nutrient release and buffering properties of the OCIO in a sustained manner.

Table 5.8: Effect of OCIO on changes of pH, Available N, sulphate, and Fe content in $(NH_4)_2SO_4$ mixed solutions

	Treatment	Duration				
		24 hours	48 hours	7 day	14 day	21 day
pH	OCIO	9.86±0.5	9.77±0.4	9.54±0.6	9.31±0.2	9.1±0.3
	Fe-EDTA	9.57±0.5	9.56±0.1	9.52±0.3	9.43±0.3	9.49±0.3
	Fe-oxalate	9.79±0.5	9.76±0.8	9.71±0.6	9.68±0.4	9.64±0.4
	$FeSO_4$	9.57±0.1	9.55±0.2	9.52±0.2	9.5±0.2	9.48±0.2
Avl N (mg L^{-1})	OCIO	661±23	936.8±23	1514.8±31	1563.8±28	1987±27
	Fe-EDTA	326.7±16	513.3±19	840±28	916.5±26	973.3±34
	Fe-oxalate	311±11	426±13	568±21	687±23	759±16
	$FeSO_4$	326.7±16	560±19	840±35	916±24	1026.7±31
Sulphate (mg L^{-1})	OCIO	356.8±21	412±16	497.6±18	517±25	568.5±23
	Fe-EDTA	331.4±15	349.9±15	414.8±22	423.8±18	460±22
	Fe-oxalate	311±11	325±12	378±14	389±13	427±18
	$FeSO_4$	549.6±14	604.7±18	725.2±34	734.5±25	764.5±24
Fe (mg L^{-1})	OCIO	96.8±2.6	115.5±3.2	223.7±2.7	256.4±2.5	316.5±2.4
	Fe-EDTA	77.14±3	98.5±3.5	96.43±2.9	101.6±3.7	105.71±5.6
	Fe-oxalate	56±5	64.5±2.5	71.8±3.1	85.6±2.1	92.5±2.5
	$FeSO_4$	186±3.4	197.7±2.7	257.79±3.2	264.2±4.6	278.5±5.5
	pH	Avl N	Sulphate	Fe		
	P(trt)<0.01 P(d)<0.01 P(trt×d)<0.01 LSD(trt)=0.013	P(trt)<0.01 P(d)<0.01 P(trt×d)<0.01 LSD(trt)=1.11	P(trt)<0.01 P(d)<0.01 P(trt×d)<0.01 LSD(trt)=0.66	P(trt)<0.01 P(d)<0.01 P(trt×d)<0.01 LSD(trt)=0.42		

*d=day, *trt=treatment

5.4.7. Solubility pattern of elements in OCIO mixed soil through application of geochemical model visual Minteq:

The data on solubility dynamics of various ions from OCIO mixed soil is presented in Table 5.9-5.13. In addition, the Table 5.13 displays the output of the Visual Minteq model at various intervals; expressed as saturation index (SI) that explains the probable saturation of various compounds in nano-mixed soil. Overall, a steady increment in pH was recorded throughout the study period in OCIO treated soil. Correspondingly, the alkalinity of OCIO10 and OCIO20 treated soil significantly increased overtime. Whereas, the pH sharply reduced in $FeSO_4$ mixed soil with little impact on the inherent alkalinity of the soil. These results were interesting because incorporation of OCIO in lower dose (10 mg kg^{-1}) was more effective than higher doses (20 and 50 mg kg^{-1}) in regard to neutralizing potentials of OCIO. As such, this particular attribute greatly facilitated P solubilization in soil solutions spiked with OCIO10 followed by OCIO20. Similarly, NO_3^- release was also prolific in presence of OCIO10 followed by OCIO20 and OCIO50. Initially, S^{2-} and SO_4^{2-} levels in $FeSO_4$ mixed solutions were significantly high; which sharply reduced after 21 days. In contrast, the S^{2-} and SO_4^{2-} dissolution gradually but considerably increased in OCIO mixed solutions; this indicates that the inherently bound sulphurs have been slowly released from the soil in presence of OCIO.

Overall, addition of OCIO in different doses led to increment in solubility of metallic cations (Fe, Mn, and Ca), which in turn substantiated the pH balancing potentials of the synthesized materials. According to the Visual Minteq model, ionic strength of the OCIO 10 mixed solutions were greatest followed by OCIO 20 and OCIO 50 at 21st day; while the ionic strength in the $FeSO_4$ mixed solutions sharply reduced over 21 days period. The model also predicted significant accumulation of chalcopyrite; Covellite, hydroxyapatite, and vivianite in OCIO incorporated soil in the long run. However, such result is expected to differ in presence of plant roots and their exudates in soil.

Table 5.9: Impact of OCIO on solubility patterns of pH, available K, alkalinity and phosphate in soil mixed aqueous media

Treatments	Attributes											
	pH			Available K			Alkalinity			Phosphate		
	7 day	14 day	21 day	7 day	14 day	21 day	7 day	14 day	21 day	7 day	14 day	21 day
OCIO 10	5.4±0.2	5.53±0.2	5.6±0.3	79.6±4	55.5±3.1	105.8±4.6	13.3±0.8	23.3±0.5	36.7±1.9	46.52±2.5	80.45±4.1	139.7±5.1
OCIO 20	5.5±0.3	5.3±0.4	5.7±0.5	74.5±3.5	54.2±2.4	87.4±3.8	13.3±0.7	26.7±1	33.3±1	71.6±3.6	77.9±3.1	84.5±3
OCIO 50	5.4±0.5	5.6±0.6	5.7±0.6	73.9±3.1	51.1±3.8	80.1±3.8	13.3±0.6	26.7±1.2	30±1.5	62.25±3.4	67.8±3.6	72.2±3.1
$FeSO_4$	3.5±0.1	3.6±0.2	3.67±0.4	115.4±4.3	74.2±3.1	72.9±3.1	20±1.4	23.3±1.1	20±1	13.7±1.1	13.8±0.7	14.9±0.8
Control	5.03±0.3	5.1±0.4	5.2±0.5	66.1±3.1	51±3.2	69.6±3	20±1	23.3±1	20±1	26.8±1.1	28.3±1.3	35.5±1.5
P(d)		0.000			0.000			0.000			0.000	
P (trt)		0.000			0.000			0.000			0.000	
P(d×trt)		0.000			0.000			0.000			0.000	
LSD(trt)		0.044			0.329			0.237			0.385	

*d=day, *trt=treatment

Table 5.10: Impact of OCIO on solubility patterns of sulphate, sulphur, nitrate and chloride in soil mixed aqueous media

Treatments	Attributes											
	Sulphate			Sulphur			Nitrate			Chloride		
	7 day	14 day	21 day	7 day	14 day	21 day	7 day	14 day	21 day	7 day	14 day	21 day
OCIO 10	2.94±0.1	6.1±0.3	40.1±2.8	0.98±0.01	2.1±0.1	13.4±0.9	99.6±4.2	130.7±4.5	124.5±4.1	595±32	665±34	700±36
OCIO 20	2.6±0.2	17.1±1	18.02±1	0.9±0.01	5.7±0.5	6.01±0.6	105.9±5.1	124.5±4.3	115.1±4	595±33	665±36	700±31
OCIO 50	2.5±0.3	10.2±1	24.3±2.8	0.8±0.01	3.4±0.8	8.1±1	93.4±4.1	96.4±4	105.9±5	560±31	805±41	700±35
$FeSO_4$	95.9±4	52.7±3.4	56.2±3.5	32±1.6	150.9±4	18.7±1.2	68.5±3	72.5±3.4	80.9±3.5	560±32	560±31	770±36
Control	2.4±0.3	35.5±1.3	32.5±1.3	0.8±0.01	11.8±1.3	10.8±1.1	31.1±1.4	56.1±3	56.04±2.3	560±33	630±36	665±33
P(d)		0.000			0.000			0.000			0.000	
P (trt)		0.000			0.000			0.000			0.000	
P(d×trt)		0.000			0.000			0.000			0.000	
LSD(trt)		0.289			0.225			0.425			0.491	

*d=day, *trt=treatment

Table 5.11: Impact of OCIO on solubility patterns of Fe, Mn, Ca, and Mg in soil mixed aqueous media.

Treatments	Attributes											
	Fe			Mn			Ca			Mg		
	7 day	14 day	21 day	7 day	14 day	21 day	7 day	14 day	21 day	7 day	14 day	21 day
OCIO 10	16.98±0.9	25.9±1	51.7±2.8	0.22±0.05	3.5±0.01	8.6±0.4	31.32±2.1	32.11±1	64.4±3.4	8.89±0.5	8.45±0.4	3.3±0.1
OCIO 20	18.1±1	28.9±1	59.7±2.1	0.13±0.02	0.05±0.02	1.73±0.05	27.95±1.1	31.7±2	43.7±2	7.9±0.6	7.99±0.8	2.3±0.6
OCIO 50	23.57±1.1	37±1.2	62.4±4	0.32±0.05	0.07±0.001	1.3±0.2	32.52±2	31.33±2.1	47.4±3.1	10.46±1.1	8.38±0.9	2.1±0.1
$FeSO_4$	31.3±1.9	33.7±1.2	50.9±3.3	1.7±3.4	0.9±0.001	0.5±0.001	609±35	329.3±16.5	338.4±16	100±21	52.6±3.5	14.5±1.4
Control	5.1±0.3	6.1±0.5	9.6±1.1	13±1.1	1.54±0.04	10.14±1.3	39.6±1.8	31.91±1.1	52±2.9	11.4±1.1	8.2±0.5	2.2±0.1
P(d)		0.000			0.000			0.000			0.000	
P (trt)		0.000			0.000			0.000			0.000	
P(d×trt)		0.000			0.000			0.000			0.000	
LSD(trt)		0.335			0.088			0.267			0.205	

*d=day, *trt=treatment

Table 5.12: Ionic strength data of Visual Minteq

Treatments	Ionic strength		
	7 Day	14 Day	21 Day
OCIO 10	0.0109	0.0114	0.0157
OCIO 20	0.014	0.0136	0.0152
OCIO 50	0.0113	0.0139	0.0149
$FeSO_4$	0.0105	0.0101	0.009
Control	0.0109	0.0118	0.0109

Table 5.13: Saturation index of Visual Minteq output at various time intervals

	OCIO10 mg kg^{-1}		OCIO 20 mg kg^{-1}		OCIO 50 mg kg^{-1}		$FeSO_4$		Control	
	Mineral	**S. I***	**Mineral**	**S. I***	**Mineral**	**S. I***	**Mineral**	**S. I***	**Mineral**	**S. I***
7 Day	$MnHPO_4$(s)	2.87	$MnHPO_4$(s)	2.91	Chalcopyrite	22.35	$MnHPO_4$(s)	2.77	$MnHPO_4$(s)	4.37
	Vivianite	1.52	Vivianite	0.93	Covellite	14.52				
					$MnHPO_4$(s)	3.19				
					Vivianite	2.79				
14 Day	Hydroxyapatite	0.21	Chalcopyrite	22.55	Hydroxyapatite	0.75			Chalcopyrite	22.86
	$MnHPO_4$(s)	2.39	Covellite	14.83	$MnHPO_4$(s)	2.64			Covellite	15.57
			$MnHPO_4$(s)	2.22	Vivianite	0.86			$MnHPO_4$(s)	3.41
21 Day	Chalcopyrite	25.32	Cr_2O_3 (c)	0.06	Chalcopyrite	25.32	$Ca_3(PO_4)_2$ (am2)	2.71	Chalcopyrite	24.19
	Covellite	15.79	Hydroxyapatite	1.88	Covellite	15.96	$Ca_3(PO_4)_2$ (beta)	3.13	Covellite	15.21
	$Cr(OH)_3$ (am)	0.41	$MnHPO_4$(s)	4.11	Cr_2O_3 (c)	0.05	$Ca_4H(PO_4)_3{:}3H_2O$(s)	3.70	$MnHPO_4$(s)	4.43
	Cr_2O_3 (c)	1.12	Vivianite	5.22	Hydroxyapatite	1.76	$CaHPO_4$(s)	0.49	Vivianite	4.98
	$FeCr_2O_4$(s)	1.32			$MnHPO_4$(s)	3.88	$CaHPO_4{:}2H_2O$(s)	0.22		
	Hydroxyapatite	1.94			Vivianite	5.29	Chalcopyrite	26.52		
	Mackinawite	0.17					Covellite	17.67		
	$MnHPO_4$(s)	4.74					Hydroxyapatite	11.68		
	Vivianite	7.496								

*S.I= Saturation index

5.4.8. Effects of OCIO application in soil: pot culture experiment-I

5.4.8.1. Changes in soil physico-chemical characteristics

A typical alluvial soil was incubated with different levels of the synthesized material (OCIO) for 90 days. The inherent physico-chemical properties of the soil are presented in Table 5.14. Incorporation of OCIO in soil @10 mg kg^{-1} significantly reduced bulk density (BD) of the soil from 1.38 ± 0.01 g cc^{-1} to 1.29± 0.01 g cc^{-1} after 90 days (Table 5.15) ($P_{0.05}$= 0.000; LSD_{day} =0.004; $LSD_{treatment}$ =0.01). Concurrently, increment in water holding capacity of soil was significant due to OCIO application in different concentration (Table 5.15). Such increment was highest with OCIO 10 mg kg^{-1} dose followed by 20 and 50 mg kg^{-1} doses ($P_{0.05}$= 0.000; $LSD_{treatment}$= 0.22). The pH of OCIO treated soil increased by 1.03–1.04 folds to 5.67–5.70 as compared to the initial value (5.5±0.1) (Table 5.14) under various concentrations in 90 days, while sharp reduction in pH was recorded due to $FeSO_4$ application in soil (Table 5.15). Interestingly, strong correlation was recorded between pH, BD, and WHC of the soil treated with different doses of OCIO during 90 day [r: pH–BD =0.997 ($P_{0.05}$ =0.000); pH–WHC=0.998 ($P_{0.05}$ =0.000); BD–WHC=0.999 ($P_{0.05}$ =0.000)].

The SOC in the soil was originally low, which noticeably enhanced in OCIO treated soil (1.96 to 2.28 folds) irrespective of doses as compared to Fe– oxalate (1.42 to 1.61 folds) and Fe–EDTA (1.64–1.81 folds) mixed soil (Table 5.15). At the end of the study period, the SOC level in soil under various treatments was in the order: OCIO 10 mg kg^{-1}> OCIO20 mg kg^{-1} > OCIO50 mg kg^{-1}> Fe–EDTA10 mg kg^{-1}> Fe–EDTA 20 mg kg^{-1}> Fe–EDTA50 mg kg^{-1}> Fe–oxalate10 mg kg^{-1} > Fe– oxalate 20 mg kg^{-1}=Fe–oxalate50 mg kg^{-1}> $FeSO_4$ 50 mg kg^{-1} ($P_{0.05}$= 0.000, $LSD_{treatment=}$ 0.04, LSD_{day}= 0.02).

The N availability remarkably increased under OCIO application during the study period (Table 5.16). Significantly higher N availability was recorded in OCIO 10 mg kg^{-1} treated soil followed by OCIO 20 mg kg^{-1} and OCIO 50 mg kg^{-1} as compared to Fe–EDTA, Fe–oxalate, and $FeSO_4$ application in various concentrations ($P_{0.05}$=0.000; LSD_{day} =3.24; $LSD_{treatment}$ =6.19). Concurrently, urease activity in soil was greater under OCIO10 mg kg^{-1} treatment ($P_{0.05}$=0.000; $LSD_{treatment}$= 0.07). A strong positive correlation (r =0.97; P =0.000) between N availability and urease activity in soil justified the results of lab-scale soil-less experiments.

Similarly, significant increment in P availability was recorded with OCIO10 mg kg^{-1} application ($P_{0.05}$ =0.000; $LSD_{treatment}$=0.20). Moreover, Fe availability in soil significantly increased after 90 days due to incorporation of OCIO @ 50, 20 and 10 mg kg^{-1} respectively. Correspondingly, phosphatase activity was highest with 10 mg kg^{-1} application of OCIO followed by 20 and 50 mg kg^{-1} application as compared to other treatments ($P_{0.05}$=0.000; $LSD_{treatment}$= 0.14). The correlation statistics also suggested strong positive correlation between available P and phosphatase activity in OCIO treated soil (r=0.99; P value=0.000), while Fe availability were negatively correlated with both available P and phosphatase (Fe–P: r =-0.99; P=0.000 and Fe–phosphatase: r=-0.99; P=0.000).

Table 5.14: Physico-chemical characteristics of the test soil

Soil properties	Mean± Std dev
pH	5.5±0.1
Bulk density (g cc^{-1})	1.42±0.02
WHC (%)	66.5±0.4
Available P (mg kg^{-1})	44.08±1.3
Phosphatase (µg g^{-1} h^{-1})	7.85±0.2
Available N (mg kg^{-1})	280.5±0.05
Urease (µg g^{-1} h^{-1})	16±0.3
Fe (mg kg^{-1})	124.6±1.2
MBC (µg g^{-1})	58.7±2.9
SOC (%)	0.49±0.04

Table 5.15: Impact of the OCIO on changes in pH, bulk density, water holding capacity, and soil organic carbon in soil (*d=day, *trt=treatment), source: Das et al. [9]

		Treatments										
Attributes	Days	Control	OCIO 10	OCIO 20	OCIO 50	EDTA 10	EDTA 20	EDTA 50	Oxalate 10	Oxalate 20	Oxalate 50	$FeSO_4$
pH	0 D	5.51±0.02	5.52±0.01	5.51±0.01	5.5±0.01	5.45±0.01	5.48±0.02	5.43±0.02	5.43±0.01	5.43±0.01	5.46±0.01	4.5±0.09
	45D	5.48±0.02	5.61±0.01	5.64±0.01	5.62±0.05	5.43±0.01	5.45±0.02	5.44±0.04	5.41±0.01	5.44±0.03	5.45±0.01	4.33±0.01
	90D	5.52±0.02	5.67±0.01	5.7±0.03	5.69±0.05	5.45±0.01	5.55±0.01	5.51±0.03	5.44±0.02	5.49±0.02	5.5±0.02	4.3±0.02
BD	0 D	1.42±0.01	1.38±0.01	1.41±0.01	1.40±0.01	1.38±0.01	1.41±0.01	1.40±0.01	1.38±0.01	1.41±0.01	1.41±0.01	1.41±0.01
(g cc^{-1})	45D	1.39±0.01	1.35±0.01	1.38±0.01	1.35±0.01	1.36±0.01	1.40±0.01	1.38±0.01	1.39±0.01	1.40±0.01	1.40±0.01	1.40±0.01
	90D	1.42±0.01	1.29±0.01	1.34±0.01	1.33±0.01	1.41±0.01	1.44±0.01	1.45±0.01	1.42±0.01	1.44±0.01	1.45±0.01	1.43±0.01
WHC	0 D	68.02±0.41	74.45±0.57	73.05±0.67	72.05±0.48	62.39±0.62	62.56±0.4	61.94±0.9	60.34±0.65	60.57±0.8	62.04±0.14	63.03±0.47
(%)	45D	68.71±0.43	75.48±0.36	75.31±0.51	74.93±0.4	58.18±0.34	59.72±0.26	58.23±0.48	57.07±0.46	58.49±0.26	58.09±0.15	54.92±0.3
	90D	71.93±0.5	80.18±0.15	78.11±0.43	77.4±0.21	56.27±0.53	57.43±0.37	56.17±0.63	54.11±0.7	54.86±0.29	55.77±0.25	58.94±0.61
SOC	0 D	0.48±0.01	0.5±0.02	0.52±0.02	0.55±0.01	0.43±0.02	0.44±0.01	0.45±0.01	0.44±0.01	0.45±0.02	0.45±0.01	0.48±0.03
(%)	45D	0.64±0.02	0.89±0.01	0.9±0.01	0.84±0.02	0.64±0.01	0.69±0.02	0.62±0.01	0.61±0.01	0.6±0.02	0.58±0.02	0.73±0.01
	90D	0.73±0.02	1.14±0.02	1.12±0.02	1.08±0.02	0.78±0.04	0.76±0.01	0.74±0.05	0.71±0.02	0.64±0.02	0.64±0.02	0.60±0.01
		pH		BD		WHC		SOC				
P value		$P_{0.05}$=0.000		$P_{0.05}$=0.000		$P_{0.05}$=0.000		$P_{0.05}$=0.000				
LSD		LSD(d)=0.022		LSD(d)=0.004		LSD(d)=0.12		LSD(d)=0.02				
		LSD(trt)=0.04		LSD(trt)=0.01		LSD(trt)=0.22		LSD(trt)=0.04				

Table 5.16: Impact of the OCIO on changes in available N, available P, DTPA extractable Fe, urease, and phosphatase activity in soil (*d=day, *trt=treatment), source: Das et al. [9]

		Treatments										
Attributes	Days	Control	OCIO 10	OCIO 20	OCIO 50	EDTA 10	EDTA 20	EDTA 50	Oxalate 10	Oxalate 20	Oxalate 50	$FeSO_4$
Avl N	0 D	282.7±3.3	287.6±7.03	284.4±5.6	282.53±4.3	280±5.4	284.66±8	289.33±6.1	275.67±8.6	280±4	280.67±8	283.6±1.6
(mg kg^{-1})	45D	291.07±4.7	381.27±2.7	372.87±6.7	374.73±9.1	279.53±9.6	284.2±7.3	284.67±3.4	275.35±4.9	278.15±3.2	279.05±8.4	297.27±2.4
	90D	299.47±3.2	387.33±3.2	384.53±6.5	381.73±9	290.26±9	281.87±1.6	287.47±2.9	284.7±8.1	275.3±8	281.9±4	280±8
Avl P	0 D	46.05±0.63	49.64±0.87	46.98±0.79	46.23±0.98	43±0.85	42.16±1.09	42.69±0.55	40.77±0.63	38.37±0.8	40.76±0.96	44.15±0.54
(mg kg^{-1})	45D	51.91±0.47	74.92±0.41	72.97±0.87	78.76±0.94	42±0.71	41.73±0.77	39.79±0.84	39.57±0.71	37.83±0.35	38.76±0.59	42.54±0.87
	90D	58.73±0.86	105.54±1.3	91.77±1.5	88.28±0.81	45.18±0.89	45.24±0.85	45.75±0.43	42.28±0.82	41.94±0.77	42.09±0.64	40.12±0.93
Urease	0 D	16.08±0.05	18.81±0.01	17.98±0.01	17.65±0.03	16.89±0.04	16.45±0.23	16.61±0.04	16.51±0.03	16.08±0.7	16.23±0.05	16.34±0.02
(µg $g^{-1}h^{-1}$)	45D	16.29±0.07	29.78±0.07	28.15±0.06	23.39±0.05	16.97±0.07	18.03±0.11	16.95±0.05	16.8±0.06	17.13±0.05	16.37±0.08	16.38±0.06
	90D	18.89±0.02	32.36±0.09	31.38±0.03	30.99±0.07	20.71±0.03	20.11±0.04	19.54±0.11	19.11±0.05	18.6±0.18	17.57±0.14	19.41±0.02
Phosphatase	0 D	7.9±0.15	12.82±0.5	11.89±0.12	10.65±0.09	8.1±0.04	7.96±0.77	7.95±0.66	7.95±0.14	7.75±0.34	7.3±0.32	8.09±0.06
(µg g^{-1} h^{-1})	45D	7.2±0.39	19.8±0.19	19.56±0.39	17.54±0.27	8.18±0.49	8.08±0.34	8.11±0.35	8.08±0.09	7.83±0.05	7.44±0.06	7.8±0.11
	90D	8.86±0.11	27.5±0.16	24.14±0.41	22.85±0.11	8.56±0.29	8.24±0.05	8.32±0.04	8.36±0.11	7.94±0.04	7.62±0.02	7.4±0.2
Fe	0 D	124±2.1	136.25±1.4	134±2.6	136.1±2.7	119.4±1.8	121.5±1.1	122.8±1.4	123.5±0.9	120.8±1.4	124.68±0.9	168.95±1.8
(mg kg^{-1})	45D	126.05±2.04	151.5±2.3	154.9±1.4	138.2±1.9	92.05±1.1	93.4±1.3	95.5±1.01	97.2±1.1	92.59±1	100.14±0.9	196.9±1.6
	90D	128.4±1.21	173.88±1.1	179.1±1.01	183.1±5.1	69.4±1.2	71.5±1.1	73.9±1.1	74.27±0.9	77.05±3.5	78.2±1.9	174.9±1.3

	Avl N	Avl P	Urease	Phosphatase	Fe
P value	$P_{0.05}$=0.000	$P_{0.05}$=0.000	$P_{0.05}$=0.000	$P_{0.05}$=0.000	$P_{0.05}$=0.000
LSD	LSD(d)=3.24	LSD(d)=0.12	LSD(d)=0.03	LSD(d)=0.07	LSD(d)=0.43
	LSD(trt)=6.19	LSD(trt)=0.20	LSD(trt)=0.07	LSD(trt)=0.14	LSD(trt)=0.83

5.4.8.2. Particle size (hydrodynamic diameter (HDD)), charge (ζ-potential), surface area, and cation exchange capacity (CEC) of OCIO spiked soil

The surface area of the OCIO spiked soil was significantly greater than Fe-EDTA and the control soil (Table 5.17); may be due to the inherently high surface area of the OCIO material (55.2 $m^2 g^{-1}$) (Fig 5.3). The ζ-potential of OCIO treated soil samples were positive and such electro positivity increased with time. The soil solids mostly carry ionic double layer owing to the adsorbed ions (cations/anions). Hence, it appears from the result that the OCIO treated soils were holding more cations than the soils under other treatments. Correspondingly, the CEC of the OCIO treated soil was significantly greater than Fe-EDTA, $FeSO_4$, treated soil samples at the time of sampling; after 90 days of incubation the cation exchange capacity of the soil were in the order: OCIO10>OCIO50>Fe-EDTA>$FeSO_4$>control ($P<0.01$, $LSD_{treatment}=0.54$). Interestingly, low dose (10 mg kg^{-1}) application of OCIO induced greater electro positivity (+ve ζ-potential) in soil than the high (50 mg kg^{-1}) application presumably due to the agglomeration tendency of the nanomaterial at high concentrations. This hypothesis was also substantiated from the DLS output. In fact, the particle size (i.e., HDD) of the OCIO spiked soil sharply reduced with time as compared to other treatments; and at 90 days, HDD of the soil under various treatments was in the order: OCIO10=OCIO 50>$FeSO_4$>Fe-EDTA>Control ($P<0.01$, $LSD_{treatment}=0.025$).

Table 5.17: Zeta potential, hydrodynamic diameter, cation exchange capacity, and surface area of soil treated with OCIO

	OCIO 10	OCIO 50	$FeSO_4$ 50	Fe-EDTA 50	Control
Days			**Zeta Potential (mv)**		
0 Day	3±0.17	1±0.17	-2	-1.1	-1.9
45 Day	5.3±0.23	1.9±0.17	0.1±0.002	0.1±0.002	-0.6
90 Day	9.2±0.8	8.3±0.9	-1.1	-0.1	-1.3
			Hydrodynamic diameter (nm)		
0 Day	0.07±0.02	0.001±0.0005	0.20±0.05	0.16±0.02	0.001±0.0001
45 Day	0.0009±0.0001	0.001±0.0005	0.531±0.08	0.436±0.02	0.001±0.0005
90 Day	0.0009±0.0001	0.0009±0.0001	1.6±0.08	0.841±0.13	0.095±0.005
			Cation exchange capacity (meq 100 g^{-1})		
0 Day	43.56±4.5	42.18±2.1	30.45±2.0	35.89±2.55	30.13±1.7
90 Day	48.75±3.2	45.23±2.8	31.57±2.3	37.8±2.25	33.45±2.1
		OCIO 10	**Fe-EDTA 10**	**Control**	
			Surface area (m^2g^{-1})		
90 Day		22.5±0.65	7.9±0.37	8.4±0.45	
	HDD	**Zeta potential**	**CEC**	**Surface area**	
P (d)	0.000	0.000	0.000		
P (trt)	0.000	0.000	0.000	0.000	
P (d×trt)	0.000	0.000	0.01		
LSD (trt)	0.025	0.068	0.54	0.079	

*d=day,*trt=treatment

5.4.9. Pot culture experiment-II: deficiency recovery potential

The changes in nutrient levels in the leached soil are presented in Fig. 5.9 a–b. Significant rise in soil pH was observed under OCIO, whereas, slight reduction in soil pH was recorded under Fe–EDTA, Fe–oxalate, and $FeSO_4$ ($P_{0.05}$=0.000; LSD=0.13). Moreover, remarkable gain in available P, phosphatase, and Fe availability occurred in OCIO treated soil as compared to the initial value (Fig. 5.9 a). Interestingly, we recorded significantly higher uptake of P and Fe in tomato plants treated with OCIO as compared to others (Fig. 5.9 b). Interestingly, the plants under OCIO treatment did not show leaf chlorosis as noted for $FeSO_4$ treated plants (Fig. 5.10). Interveinal chlorosis is a definite symptom of Fe deficiency. Moreover, we recorded a significantly high tomato yield in OCIO treated plants (Fig. 5.9 b). This signifies that the synthesized material was not only efficient in recovering Fe and P fertility in soil but also greatly facilitated plant growth and productivity. On the whole, the results of

soil and plant experiments indicated that the efficiency of OCIO was highest when applied @10 mg kg^{-1}.

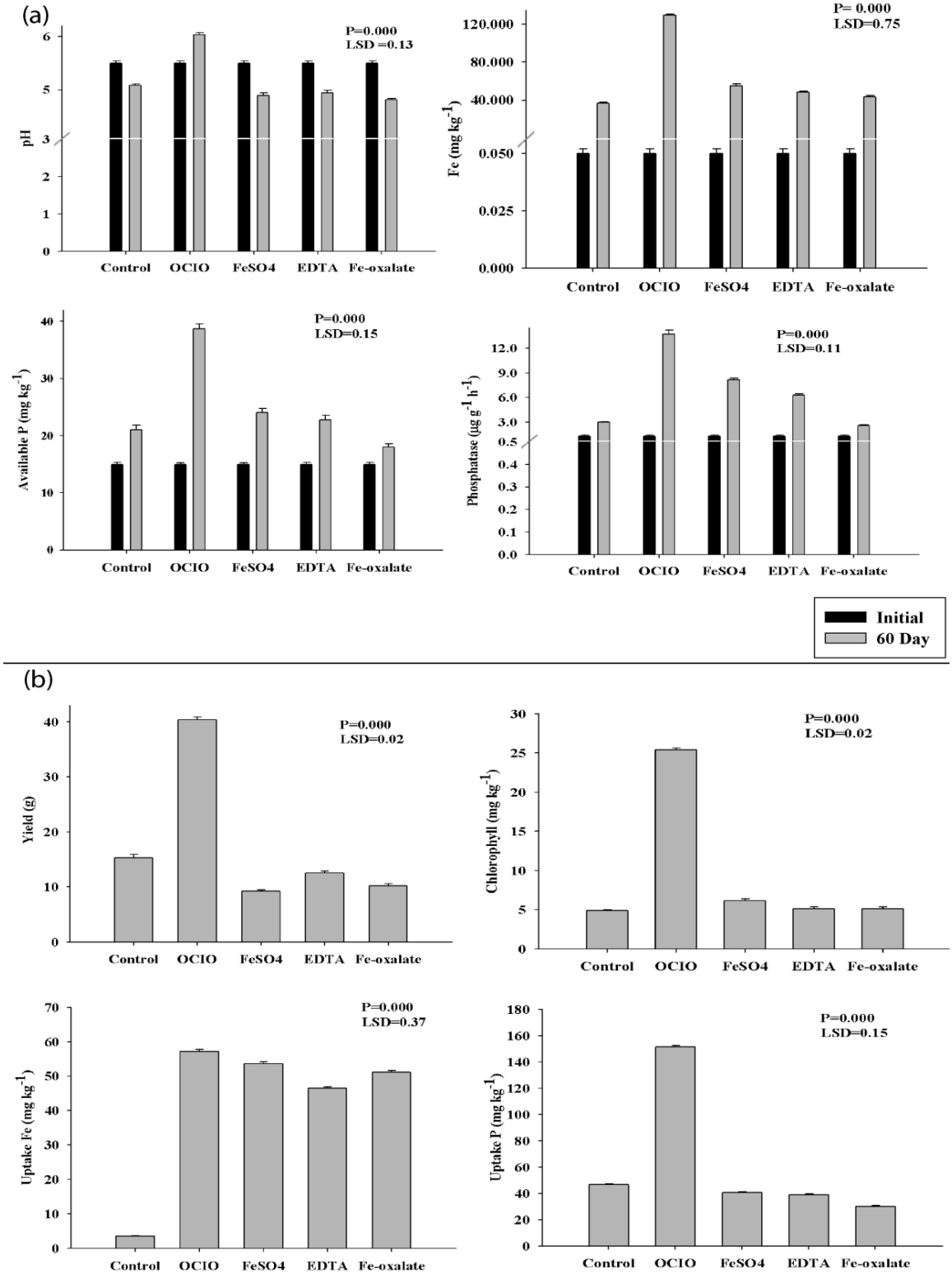

Fig. 5.9: (a): Changes in pH, Avl P, phosphatase activity, Fe content in leached soil; (b): uptake of P and Fe, Chlorophyll content & yield in leached plant, source: Das et al. [9]

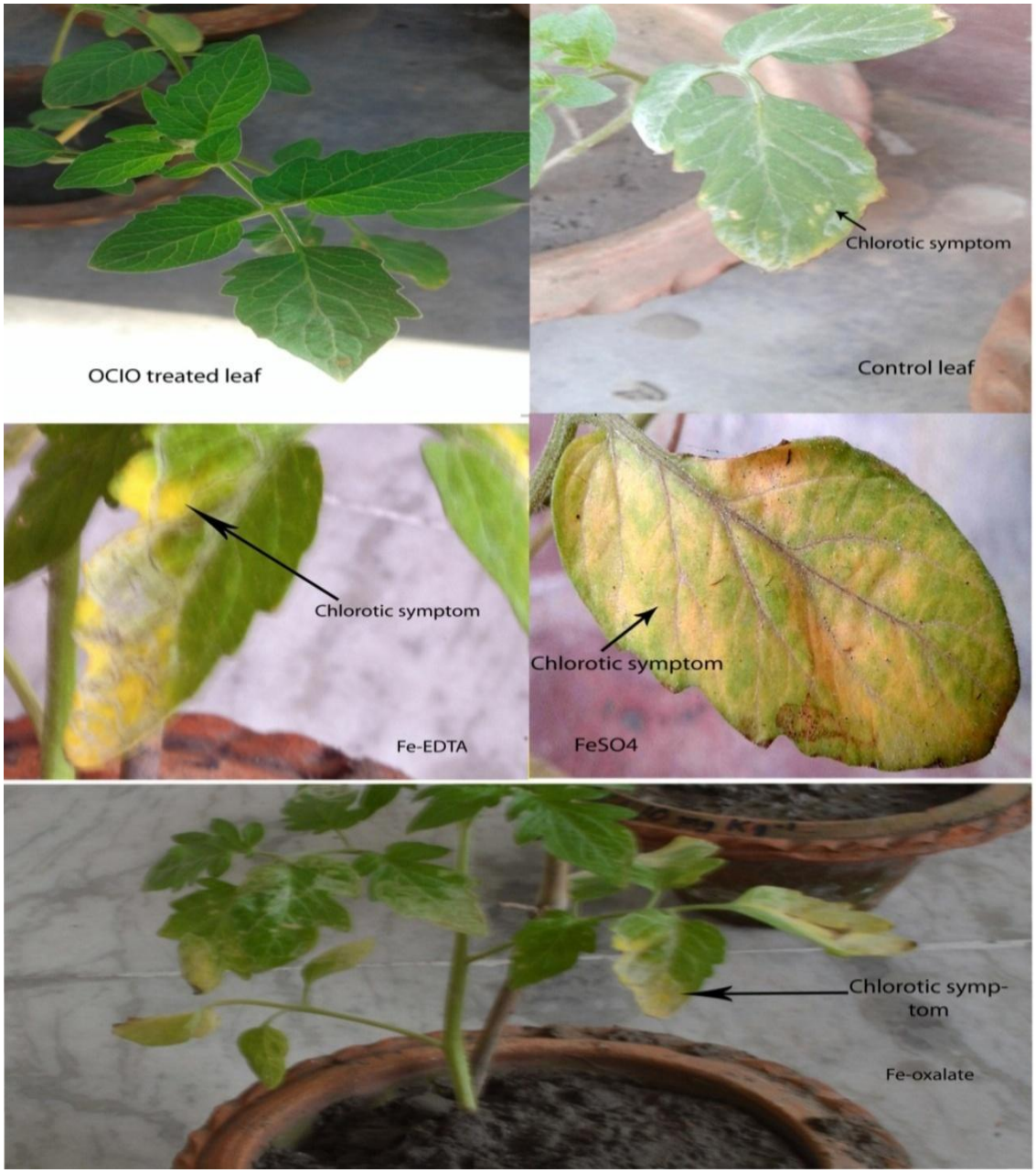

Fig. 5.10: Leaf chlorotic symptoms in control, Fe-EDTA, Fe-oxalate and $FeSO_4$ treatments, source: Das et al. [9]

5.4.10. Field experiment: Impact on large scale application

5.4.10.1 Impacts on field soil fertility

The inherent properties of the soil have been presented in Table 5.18. The soil organic carbon content of the soil was inherently about 0.7%, which significantly increased in OCIO treated plots under tomato cultivation. After two years of cultivation, about 1.5-1.9 folds increment was recorded in OCIO treated plots (Table 5.19). SOC content was significantly high in OCIO 2 kg ha^{-1} treated plots followed by OCIO 5 and 10 kg ha^{-1} treatments (P(trt)<0.01; LSD=0.04). Similarly, MBC and MBN levels in OCIO 2 kg ha^{-1} treated plots significantly improved over years as compared to other treatments (Table 5.19). In fact, MBC and MBN levels marginally reduced in plots treated with $FeSO_4$ for two years. Overall the results implied that the SOC gain in OCIO treated plots was largely due to the augmentation of the microbial biomass and their activity in OCIO treated plots.

The characteristic relationships between soil pH and Fe release from OCIO in tomato field exhibited a close resemblance with the lab based experiments. The pH of the tomato soil significantly increased under various doses of OCIO over two years. The acidifying effect of Fe-EDTA and $FeSO_4$ was evidenced in both the years. At the end of the second year of cultivation, Fe bioavailability was: OCIO 20 kg ha^{-1}> OCIO 10 kg ha^{-1}> OCIO 5 kg ha^{-1}> OCIO 2 kg ha^{-1}>$FeSO_4$ 20 kg ha^{-1}>Fe-EDTA 20 kg ha^{-1}> Fe-EDTA 10 kg ha^{-1}> Fe-EDTA 5 kg ha^{-1}>Fe-EDTA 2 kg ha^{-1} (Table 5.20; P(trt)<0.01; LSD=1.47).

Table 5.18: Physico-chemical characteristics of the test soil under field condition

Soil properties	Mean± Std dev
pH	5.0±0.2
Available P (mg kg^{-1})	18.54±1.1
Phosphatase (µg g^{-1} h^{-1})	21.15±0.2
Available N (mg kg^{-1})	195±0.02
TKN (%)	1.21±0.5
Available K (mg kg^{-1})	48.3±0.8
Urease (µg g^{-1} h^{-1})	18.1±0.3
Fe (mg kg^{-1})	48.4±1.1
MBC (µg g^{-1})	26.7±2.1
SOC (%)	0.7±0.05

Table 5.19: Impact of OCIO on Soil organic carbon, MBC, and MBN content of field condition soil

	Soil organic carbon (%)		MBC (µg g^{-1})		MBN (µg g^{-1})	
Treatments	First yr	Second yr	First yr	Second yr	First yr	Second yr
Control	0.74±0.02	0.92±0.05	34.93±2.26	28.72±2.1	5.18±0.3	4.26±0.3
OCIO 2	1.16±0.02	2.06±0.05	49.23±1.23	69.94±1.3	7.31±0.6	10.38±0.2
OCIO 5	1.09±0.04	2.02±0.06	45.71±1.06	65.25±1.3	6.78±0.6	9.68±0.2
OCIO 10	1.09±0.05	1.99±0.05	45.71±1.23	64.86±1.3	6.78±0.6	9.62±0.2
OCIO 20	1.07±0.06	1.92±0.05	41.42±1.44	59.39±0.6	6.15±0.3	8.81±0.1
Fe-EDTA 2	0.77±0.05	0.95±0.04	35.55±1.7	31.65±3.1	5.28±0.4	4.69±0.4
Fe-EDTA 5	0.77±0.04	0.96±0.04	35.55±1.9	29.3±2	5.28±0.4	4.35±0.3
Fe-EDTA 10	0.75±0.05	0.92±0.04	33.6±0.7	30.08±0.7	4.99±0.4	4.46±0.1
Fe-EDTA 20	0.71±0.06	0.85±0.04	30.87±1.1	28.52±0.5	4.58±0.6	4.23±0.5
$FeSO_4$ 20	0.74±0.05	0.92±0.04	30.48±1.1	26.26±0.3	4.52±0.4	3.89±0.6
P (yr)	<0.01		<0.01		<0.01	
P (trt)	<0.01		<0.01		<0.01	
P (yr×trt)	<0.01		<0.01		<0.01	
LSD (trt)	0.04		1.68		0.25	

Table 5.20: Impact of OCIO on pH and Fe availability of field condition soil

Treatments	pH		Available Fe (mg kg^{-1})	
	First yr	Second yr	First yr	Second yr
Control	5.2±0.03	5.34±0.09	52.4±1.2	58.8±1.5
OCIO 2	5.84±0.03	5.96±0.05	115.12±1.1	148.1±2.1
OCIO 5	5.81±0.02	5.89±0.04	129.56±1.7	162.1±1.9
OCIO 10	5.78±0.05	5.81±0.04	134±1.3	179.85±2.5
OCIO 20	5.56±0.02	5.62±0.02	152.56±1.7	189.34±1.4
Fe-EDTA 2	5.04±0.03	4.97±0.05	63.4±1.7	72±1.8
Fe-EDTA 5	5.01±0.05	4.85±0.04	65.96±1.2	80.7±1.8
Fe-EDTA 10	5.02±0.05	4.81±0.05	69.48±1.7	83±1.7
Fe-EDTA 20	4.96±0.04	4.75±0.04	72.24±1.1	90.4±1.5
$FeSO_4$ 20	4.48±0.03	4.41±0.07	80.3±1.1	108.8±1.2
P (yr)	<0.01		<0.01	
P (trt)	<0.01		<0.01	
P (yr×trt)	<0.01		<0.01	
LSD (trt)	0.02		1.47	

About by 1.9-2.6 folds increment in both total N and mineralizable-N content of the soil was evidenced due to OCIO 2 kg ha^{-1} and OCIO 5 kg ha^{-1} application as compared to the initial values. Urease activity was significantly high with OCIO 2 kg

ha^{-1} followed by OCIO 5 kg ha^{-1}, OCIO 10 kg ha^{-1} application (P(trt)<0.01; LSD(trt)=1.27).

Table 5.21: Impact of OCIO on available N, total N, and urease activity of field condition soil

Treatments	Available N ($mg\ kg^{-1}$)		Urease activity ($\mu g\ g^{-1}h^{-1}$)		TKN (%)	
	First yr	Second yr	First yr	Second yr	First yr	Second yr
Control	221.2±10	262.27±16	24.51±1.1	27.89±1.2	1.23±0.1	1.36±0.3
OCIO 2	297.73±14	388.27±12	58.74±1.5	71±2.6	2.01±0.4	3.17±0.4
OCIO 5	285.6±15	384.53±10	54.51±2.5	61.04±2.7	1.94±0.5	2.9±0.4
OCIO 10	281.87±19	382.67±14	47.3±2.1	54.55±3	1.92±0.5	2.85±0.4
OCIO 20	282.8±15	365.87±16	41.48±2	47.45±3.2	1.76±0.6	2.11±0.5
Fe-EDTA 2	219.3±16	191.3±18	19.12±1.4	15.96±1.1	1.16±0.4	1.43±0.6
Fe-EDTA5	199.73±16	186.67±15	18.45±1.5	14.14±1.1	1.29±0.6	1.36±0.4
Fe-EDTA 10	196±25	178.27±15	16.79±1	13.23±1.2	1.26±0.4	1.41±0.4
Fe-EDTA 20	172.67±16	161.47±17	15.17±1	13.76±1.1	1.27±0.6	1.57±0.5
$FeSO_4$ 20	200.67±16	181.07±12	14.77±1.1	13.81±2.1	1.14±0.6	1.51±0.6
P (yr)	<0.01		<0.01		<0.01	
P (trt)	<0.01		<0.01		<0.01	
P (yr×trt)	<0.01		<0.01		<0.01	
LSD (trt)	6.19		1.27		0.040	

The P availability in soil significantly improved due to OCIO 2 kg ha^{-1} application followed by OCIO 5 kg ha^{-1} and OCIO 10 kg ha^{-1} (P(trt)<0.01; LSD(trt)=0.09); strong positive correlation between P increment patterns in aqueous medium, in soil under laboratory condition was also detected. Consequently, the K availability in cultivated soils significantly improved due to OCIO 2 kg ha^{-1} application followed by OCIO 5 kg ha^{-1}, OCIO 10 kg ha^{-1}, and OCIO 20 kg ha^{-1} (P(trt)<0.01; LSD(trt)=0.22). Moreover, we recorded strong positive correlation between the K release profile in aqueous solution and in soil under laboratory condition. Moreover, we recorded remarkable phosphatase activity under OCIO 2 kg ha^{-1} followed by OCIO 5 kg ha^{-1} and OCIO 10 kg ha^{-1} treatments in soil after second year of crop cultivation. Overall, The 2 kg ha^{-1} dose was found to be most efficient among all the doses used in this experiment.

Table 5.22: Impact of OCIO on available P and phosphatase activity of field condition soil

Treatments	Available P (mg kg^{-1})		Phosphatase activity (µg $g^{-1}h^{-1}$)		Available K (mg kg^{-1})	
	First yr	Second yr	First yr	Second yr	First yr	Second yr
Control	22.51±0.2	29.81±1.3	22.38±1	30.77±1	56.37±8	65.5±5
OCIO 2	67.53±2.1	96.07±2.1	37.74±1.1	57.02±1.1	108.7±10	212±22
OCIO 5	51.89±1.5	76.45±2.1	35.9±1.3	52.09±1.1	105.2±12	208±24
OCIO 10	46.55±1.1	71.1±2.1	31.7±0.71	48.69±0.41	101±11	182.43±11
OCIO 20	41.86±1.1	59.31±2.1	30.17±0.21	45.12±0.25	81.47±6	160.87±12
Fe-EDTA 2	24.05±1.3	31.52±2.2	20.38±1.2	18.6±0.94	56.73±4	88.4±8
Fe-EDTA 5	23.49±1.4	30.22±1.1	18.67±0.8	16.55±0.21	55.8±2	87.97±7
Fe-EDTA 10	21.48±1.1	27.24±1.1	17.12±0.9	16.02±0.74	50.8±3	97.03±8
Fe-EDTA 20	20.25±1	25.09±1.3	16.9±0.7	16.19±0.55	42.23±2.5	69.13±5
$FeSO_4$ 20	19.99±1	22.35±1.2	18.71±0.9	17.76±0.5	40.07±2.3	79.73±8
P (yr)	<0.01		<0.01		<0.01	
P (trt)	<0.01		<0.01		<0.01	
P (yr×trt)	<0.01		<0.01		<0.01	
LSD (trt)	0.09		0.88		0.22	

5.4.10.2. Impacts on crop

The OCIO [Fe(ox)-Fe_3O_4] were field tested on tomato. Four doses (2, 5, 10, and 20 kg ha^{-1}) of the prepared compound was selected for this study and compared with Fe-EDTA (2, 5, 10, and 20 kg ha^{-1}) and $FeSO_4$ @ 20 kg ha^{-1} (recommended dose) used as control. All other agronomic management practices such as seed treatment, land preparation, fertilizer (NPK) application, intercultural operation, and pest control measures were uniformly conducted for all the treatments following the package of practice recommended by the Department of Agriculture, Govt. of Assam. The study was conducted in a randomized block design with four replicates.

Following are the major results of the field trials:

Although several growth and yield attributes were analyzed, considering the large volume of the thesis only most vital outcomes are presented here. The Chlorophyll content in tomato leaves was significantly high when OCIO was applied as 2 kg ha^{-1} (48.59± 0.13 mg g^{-1} leaves) during the first year of cultivation. Likewise, 10 kg ha^{-1} dose for OCIO also showed good chlorophyll content (47.65± 0.52 mg g^{-1}). Moreover,

the Carotenoid content in tomato was significantly high under 5 kg ha^{-1} dose of OCIO (10.26± 0.33 mg g^{-1}) during the first year of cultivation. In addition OCIO @ 2 and 10 kg ha^{-1} also attributed high carotenoid content in tomato (7.43±0.18 and 8.61±0.05 mg g^{-1}) respectively (Table 5.23).

Table 5.23: Impact of OCIO on chlorophyll and carotenoid content

	Total chlorophyll (mg g^{-1})		Carotenoid (mg g^{-1})	
Treatment	First yr	Second yr	First yr	Second yr
Control	23.65±0.1	27.89±0.03	3.33±0.03	3.14±0.01
OCIO 2	48.59±0.13	59.57±0.9	7.43±0.18	4.38±0.5
OCIO 5	38.19±0.15	52.34±0.2	10.26±0.33	2.08±0.05
OCIO 10	47.65±0.52	51.75±0.1	8.61±0.05	10.66±0.05
OCIO 20	23±0.02	49.89±0.1	3.28±0.2	4.18±0.12
Fe-EDTA 2	16.25±0.03	25.01±0.2	3.58±0.16	3.7±0.14
Fe-EDTA 5	16.77±0.3	23.88±0.2	2.03±0.11	3.01±0.12
Fe-EDTA 10	18.87±0.2	22.5±0.3	2.69±0.48	4.41±0.19
Fe-EDTA 20	19.64±0.04	27.93±0.1	3.75±0.09	3.36±0.03
FeSO4	16.14±0.01	16.14±0.01	4.55±0.01	4.55±0.01
P (yr)	<0.01		<0.01	
P (trt)	<0.01		<0.01	
P (yr×trt)	<0.01		<0.01	
LSD (trt)	0.16		0.13	

Maximum yield of tomato was obtained under 2 kg ha^{-1} (41.67±1.11 tonne ha^{-1}) followed by 5 kg ha^{-1} (38.3±2.4 tonne ha^{-1}) application of OCIO compound (Table 5.24), which are almost 2.49 and 2.29 folds higher than the yield obtained with 20 kg ha^{-1} of $FeSO_4$ (16.7±0.2 tonne ha^{-1}) application. Tomato yield under 2 kg ha^{-1} application of OCIO was significantly higher than the yield under 10 kg ha^{-1} Fe-EDTA (20.75±2.7 tonne ha^{-1}) application (P(trt) <0.01; LSD(trt) =0.03). Moreover, at the end of second year, tomato yield was found in the order: OCIO 2 kg ha^{-1}>OCIO 5 kg ha^{-1}>OCIO 10 kg ha^{-1}> OCIO 20 kg ha^{-1}>Control>Fe-EDTA 2 kg ha^{-1}>Fe-EDTA 5 kg ha^{-1}> Fe-EDTA 10 kg ha^{-1}> Fe-EDTA 20 kg ha^{-1}>$FeSO_4$ 20 kg ha^{-1}. In addition, significantly high lycopene content was recorded in OCIO 2 kg ha^{-1} treated tomatoes followed by OCIO 5 kg ha^{-1}, OCIO 10 kg ha^{-1}, and OCIO 20 kg ha^{-1} in both the years (P(trt) <0.01; LSD(trt) =0.02).

Table 5.24: Impact of OCIO on Lycopene content and yield of tomato grown under field condition.

Treatments	Lycopene (mg kg^{-1})		Yield (tonne ha^{-1})	
	First yr	Second yr	First yr	Second yr
Control	6.19±0.12	9.7±0.1	20±2.8	24±2.4
OCIO 2	12.48±0.1	19.19±0.1	41.67±1.1	65±1.8
OCIO 5	11.3±0.2	15.27±0.2	38.3±2.4	53.3±1.8
OCIO 10	10.56±0.2	13.26±0.3	30.67±0.8	48±1.9
OCIO 20	11.56±0.1	11.19±0.3	24.17±2.1	34.17±2
Fe-EDTA 2	10.46±0.3	8.63±0.3	20±3.1	23.8±2
Fe-EDTA 5	5.35±0.3	8.61±0.3	20.08±3.5	22.5±1.9
Fe-EDTA 10	5.19±0.2	8.35±0.3	20.75±2.7	21.5±2.1
Fe-EDTA 20	4.55±0.1	7.53±0.3	17.67±2.6	16.3±1
$FeSO_4$ 20	12.68±0.5	8.25±0.3	16.67±2.6	14.8±1.4
P (yr)	<0.01		<0.01	
P (trt)	<0.01		<0.01	
P (yr×trt)	<0.01		<0.01	
LSD (trt)	0.02		0.03	

In addition to the plant parameters discussed above, data on periodic plant height and leaf number, pericarp thickness of the tomato fruits, along with total acidity and total soluble solids were also recorded. Such results were exactly similar to the outcomes shown above. Therefore, presentation of such repetitive outcomes has been avoided here. However, these results are presented in Annexure1.

Shelf life indicates the weight loss in the harvested fruit under storage condition. It mainly gives an idea of the longevity of the fruit in storage condition. Here, shelf life was measured by recording the changes in fruit weight at an interval of 20 days in fruits stored in room-temperature. Significant weight loss in tomato was recorded under Fe-EDTA and $FeSO_4$ treatments in both the years. Moreover weight reduction in tomato was more prominent in second year crop as compared to first year under Fe-EDTA and $FeSO_4$ treatments. In contrast, weight reduction of the OCIO treated fruits was marginal (1.25-1.57 folds) (Fig. 5.11). However, the weight of Fe-EDTA (20 kg ha^{-1}) treated fruits drastically reduced by 1.99 folds in 60 days. Similarly, 2.48 folds reduction in fruit weight was recorded in $FeSO_4$ treated fruits.

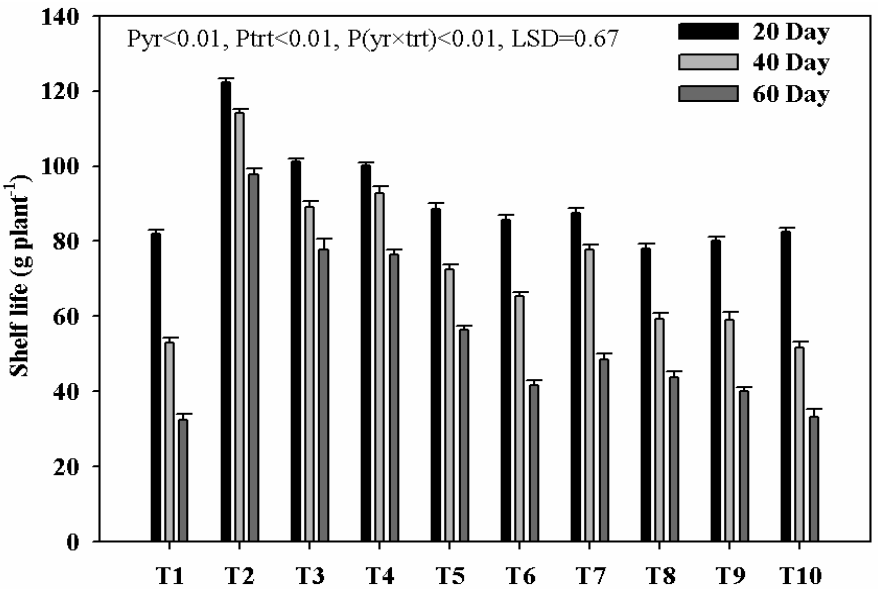

Fig. 5.11: Impact of OCIO on shelf life of tomato grown under field condition

T1=Control, T2=OCIO 2kg ha^{-1}, T3=OCIO 5 kg ha^{-1}, T4=OCIO 10 kg ha^{-1}, T5= OCIO 20 kg ha^{-1}, T6=Fe-EDTA 2 kg ha^{-1}, T7=Fe-EDTA 5 kg ha^{-1}, T8=Fe-EDTA 10 kg ha^{-1}, T9=Fe-EDTA 20 kg ha^{-1}, T10=$FeSO_4$ (*yr=year, *trt=treatment)

The rate of oxygen evolution in hill reaction was also noteworthy in OCIO treated plants (P<0.01, LSD=64) (Table 5.25). Moreover, the photosynthetic rate (i.e., µM CO_2 assimilation per unit area and time) was remarkable under OCIO followed by Fe-EDTA and $FeSO_4$ treated plants (P<0.01, LSD=0.2) (Table 5.25). Nitrate reductase (NR), glutamine synthetase (GS), and glutamate synthase (GOGAT) are the prime enzymes in N assimilation and amino acid production in plant. Significantly higher NR activity was observed in OCIO treated plants as compared to Fe-EDTA, $FeSO_4$ and control (Table 5.26). Remarkably high GS and GOGAT activity in OCIO treated tomato leaves was recorded as compared to Fe-EDTA, $FeSO_4$, and control (Table 5.26). The *GOGAT* gene in tomato was upregulated under OCIO than Fe-EDTA treatment. Similarly, the upregulation of the *GS2* gene was also significantly greater under OCIO than Fe-EDTA (Table 5.27).

Table 5.25: Effect of OCIO on hill activity and photosynthetic rate in tomato grown under field condition

Treatment	Attributes	
	Hill activity	PSR
	($\mu M\ h^{-1}$)	($\mu M\ CO_2\ m^{-2}\ s^{-1}$)
	Mean±stdev	Mean±stdev
Control	4085.5±102	28.19±1.1
OCIO	6621.6±212	60.56±1.8
Fe-EDTA	4106.6±115	24.11±1.7
$FeSO_4$	4218.3±103	21.65±1.0
P value	<0.01	<0.01
LSD	64	0.2

Table 5.26: Effect of OCIO on NR, GS, and GOGAT activity in tomato grown in field condition

Treatment	Attributes		
	NR	GS	GOGAT
	($g\ h^{-1}$)	($\mu M\ min^{-1}\ g^{-1}$)	($nM\ min^{-1} mg^{-1}$)
	Mean±stdev	Mean±stdev	Mean±stdev
Control	30.81±1.5	0.003±0.0005	12.2±0.8
OCIO	49.78±1.3	0.06±0.001	19.64±0.5
Fe-EDTA	24.41±1.1	0.001±0.0004	10.02±0.6
$FeSO_4$	32.68±1.3	0.0011±0.0004	11.11±1.1
P value	<0.01	<0.01	0.06
LSD	0.1	0.023	0.01

Table 5.27: Effect of OCIO on *NR*, *GS2*, *GOGAT*, and *Fd* gene in tomato grown in field condition

Treatment	Attributes			
	NR	*GOGAT*	*GS2*	*Fd*
	Mean±stdev	Mean±stdev	Mean±stdev	Mean±stdev
Control	1±0.1	1±0.01	1±0.005	1±0.005
OCIO	2.08±0.1	1.72±0.17	4.57±0.03	14.22±1
Fe-EDTA	0.38±0.07	0.005±0.0001	0.52±0.005	0.03±0.001
$FeSO_4$	0.88±0.09	0.26±0.03	0.58±0.005	0.53±0.03
P value	<0.01	<0.01	<0.01	<0.01
LSD	0.074	0.074	0.07	0.24

Correspondingly, N and P uptake was greater in OCIO treated tomato as compared to Fe-EDTA and $FeSO_4$ ($P<0.01$; N: LSD=0.01, P: LSD=0.03) (Table 5.28).

Eventually, Fe uptake was also remarkably higher in plants treated with OCIO as compared to Fe-EDTA, $FeSO_4$, and control.

Table 5.28: Effect on uptake of N, P, and Fe of tomato grown in field condition

Treatment	Attributes		
	Uptake N (%) Mean±stdev	Uptake P ($mg\ kg^{-1}$) Mean±stdev	Uptake Fe ($mg\ kg^{-1}$) Mean±stdev
Control	1.5±0.5	22.11±1.1	38.45±2.1
OCIO	2.8±0.5	104.34±5.6	108.85±11.4
Fe-EDTA	1.1±0.01	45.14±2.5	55.14±2.1
$FeSO_4$	0.9±0.001	65.17±4.1	88.31±3.5
P value	<0.01	<0.01	<0.01
LSD	0.01	0.03	0.69

Table 5.29 represented the data of catalase, super oxide dismutase, and lipid peroxidation. In plant cells the activities of catalase and SOD induced in presence of oxidative stress to counter it. Here in this study we recorded significantly higher catalase activity in Fe-EDTA and $FeSO_4$ treatment. Likewise, malondehyde production through lipid peroxidation indicates cell damage. Lipid peroxidation was significantly higher in $FeSO_4$ and Fe-EDTA. SOD activity was highest under Fe-EDTA followed by untreated and $FeSO_4$ treatment ($P<0.01$; LSD=0.13). Moreover, low level of catalase, SOD activity, and lipid peroxidation were recorded in OCIO treated plants which indicated the eco friendly nature of our synthesized material.

Table 5.29: Effect of OCIO on catalase, lipid peroxidation, and super oxide dismutase activity in leaves of tomato grown in field condition

Treatment	Attributes		
	Catalase ($mL\ min^{-1}g^{-1}$) Mean±stdev	Lipid peroxidation (μMg^{-1}) Mean±stdev	SOD ($min^{-1}\ mg^{-1}$) Mean±stdev
Control	7.9±0.8	0.008±0.001	30.87±1.1
OCIO	5.3±1.1	0.002±0.001	9.9±1
Fe-EDTA	9.3±0.5	0.011±0.001	32.4±1.2
$FeSO_4$	9.3±0.5	0.013±0.001	27.8±1.1
P value	0.3	<0.01	<0.01
LSD	2.3	0.0007	0.13

5.5. Discussions

Recently, Conway et al. [41] suggested that illumination levels and nutrient availability greatly regulate the plant-nanomaterial interaction and argued that plants are vulnerable to certain engineered nanomaterials. On the contrary, this research reveals the oxalate capped iron oxide nanomaterial that was found to be extraordinarily effective micronutrient soil conditioners through series of the soil-plant interactive experimentations. The synthesis is easy, scalable, and green for widespread use. These materials were readily soluble in water and improved soil health by i) buffering pH, ii) increasing the Fe availability without causing acidity, iii) enhancing porosity; iv) Promoting microbial diversity, and v) increasing NPK availability. The study also facilitated to appreciate the probable mechanisms of actions of the nanomaterials in soil-plant system. In soil systems both solid and aqueous phases exist along with considerable properties of natural colloidal substances [42]. Therefore, the synthesized material was exposed to both aqueous and solid (i.e., soil) medium in laboratory and in ambient conditions.

5.5.1. Environmental toxicology assessments: Impacts on earthworms, soil beneficial microorganisms and seed germination

Effects of metal oxide nanoparticles on earthworm health are largely dose dependent [13]. High dose exposure (above 400 mg kg^{-1}) induced remarkable oxidative stress in earthworms [43,44]. Earthworms have also been reported to be sensitive to zero-valent Fe [13]. In contrast, there was no evidence of oxidative stress in OCIO exposed *E. fetida*. However, the dose dependent impacts of nanomaterials in regard to expressions of oxidative stress indicators (Catalase, GSH, SOD, and lipid peroxidation) in earthworms were evidenced in our study. Overall the protein level was significantly greater in OCIO (10 mg kg^{-1}) exposed earthworms whereas, Fe accumulation in such earthworms was lower than $FeSO_4$ (50 mg kg^{-1}) exposure (Table 5.6). This indicates the efficiency of nano form Fe was greater than the other forms in regard to earthworm health and metabolism. However, this statement is subject to further in depth validation in future.

Germination study and inhibition to beneficial soil bacteria are dependable eco-toxicity analyses for nanomaterials [45, 46]. Many workers have suggested that iron nanomaterials may induce microbial toxicity by creating anoxic condition and

generating ROS [5,13]. Such condition also creates high phytotoxicity by affecting the root growth and seed germination. Fascinatingly, the OCIO did not arrest microbial proliferation in soil, had no harmful effects on beneficial bacteria, and facilitated seed germination and root-shoot development.

Contrary to our results, El-Temsah and Joner [13] reported high phytotoxicity of zero valent iron (Fe^0) nanoparticles [13]. However, such results were found only at an abnormally high dose (1000 to 5000 mg kg^{-1}) of Fe^0 nanoparticles; in fact, 100% seed germination was observed with low dose (100–200 mg kg^{-1}) in their research. Predominance of Fe^0 may create anoxic condition through their reductive reactions, which is unhealthy for plants and soil bacteria [13]. Hence, such toxic impacts could be avoided using the OCIO in our study. Generally, the inhibitory effects of Fe on root growth and germination of plant seeds is highly pronounced at low pH (2–3) condition [47]. In all probability, the unique buffering property of the OCIO (explained in the following section) helped to maintain a neutral pH of the aqueous medium that could minimize the probability of excessive Fe solubility and phytotoxicity.

The role of *Rhizobium* in *N fixation* and *S. marcescens* in P solubilization has been well documented by other workers [48,49]. Moreover, the authenticity of the germplasm of these species has been thoroughly verified in our previous study [50]. Therefore, these two species were an easy and dependable choice as models for this experiment. This property is important to evaluate the quality of the synthesized material from an ecological view point [51]. Generally, the zone of inhibition in growth medium is the indicator of fatal impact on microbial colonies for any material (Fig. 5.5a and b).

Generally, abundance of soluble iron [Fe(II)] in soil greatly activates N-fixing bacteria [52]; this study has shown that how the OCIO incorporation sustained the release of iron in bioavailable form in soil. High surface-to-volume ratio of these nano-metal oxides ensures greater partial decomposition and release of ions compared to the bulk materials [53].

5.5.2. OCIO and pH interaction: the buffering mechanism and nutrient (N, P, and Fe) availability dynamics

In general, the association of nanoparticles and pH greatly depends on colloidal stability, dominant electrolytes in the media, and capping agents [54,55]. When the OCIO was introduced to aqueous solutions of extreme pH (4 and 9), gradual to sharp shift towards neutrality was observed, while the pH of the originally neutral solution did not change. Such result suggested that the synthesized material can act as both proton donor and proton acceptor. Fe^{2+} form of iron in $FeSO_4$ resulted in rapid reduction in pH of the solutions in our experiment because $FeSO_4$ is readily hydrolysable and generates H^+ and Sulphate in solution. Moreover, P bioavailability sharply reduced in presence of $FeSO_4$ may be due to formation of insoluble iron phosphate [56]. The following reactions may take place in low pH condition in presence of $FeSO_4$:

(i) $2Fe^{2+} + 6H_2O = 2\ Fe(OH)_3 + 6H^+ + 2e^-$

Due to predominance of H^+ ions in the solution the $Fe(OH)_3$ may again undergo the following reaction –

(ii) $Fe(OH)_3 + 3H^+ = Fe^{3+} + 3H_2O$

Or the ferrous may remain partially soluble in soil solutions as proposed below:

(a) $Fe\ (OH)^+ \rightarrow Fe(OH)^{2+} + e^-$

(b) $Fe\ (OH)^0{}_2 \rightarrow Fe(OH)^+{}_2 + e-$ [57]

Interestingly, the result with OCIO was radically different. In fact, increment in pH was observed towards neutral range in acidic soil and solutions as well as uniform bioavailability of N, P, and Fe. Presumably, in low pH solution, the synthesized materials might trapped the excess H^+ in their polymeric framework, whereas, such phenomenon did not persist in high pH, due to scarcity of H^+ ion in the environment [9]. As such, the release of Fe^{2+} was greatly controlled by the Fe-oxalate: Fe_3O_4 ratio; which was found to be most effective at 3 to 7:1.

The advantage of the excellent buffering capacity of the manufactured nanomaterials could better understood in regard to P release from KH_2PO_4 solution

because there was no evidence of formation of insoluble $Fe_3(PO_4)_2$ or $FePO_4$ with OCIO. It is believed that solubility of engineered nanomaterial is pH dependent and possibly the dissolution is highly profound in acidic solutions [58,59]. The rate of dissolution is also influenced by residence time and composition of the solution Avramescu et al. [58].

5.5.3. Impact on solubility dynamics of cations and anions in OCIO mixed soil

Solubility of elemental ions chiefly governs the leaching process depending on precipitation, dissolution, and adsorption equilibrium [60]. Moreover several factors (solid matrix, nature of extractant and concentration, duration of exposure, and pH of the leachates) control the leaching pattern of metallic cations in the long run [61]. On the basis of these arguments, it was necessary to recognize the environmental consequences of nanomaterial inoculated soil. p^H varied significantly in this experiment although there was overall rise in pH in all OCIO inoculated soils. Such changes in pH significantly influence mobility of trace elements in soil [61,62]. However, rise in pH under OCIO treated soil solutions signifies that the oxalate capped Fe resisted the natural process of Fe hydrolysis in aqueous medium. Moreover, soluble compound of Mg may be one of the principle contributors of change in pH [60]. Generally SO_4^{2-}, PO_4^{3-} and NO_3^- concentrations increased in OCIO mixed solutions whereas the solubility of Mg markedly reduced. This is probably due to high affinity of Mg^{++} ion to carbonates and silicates in the soil [62]. As discussed earlier, the leaching pattern of metal ions is largely controlled by pH and alkalinity.

5.5.4. Impact on zeta potential and hydrodynamic diameter of soil

Soil is a complex and dynamic body made up of charged solid, dissolved organic and inorganic compounds, living macro and micro-biota, and gaseous substances [63]. Rarely, chemical equilibrium is reached in any soil and thus they are highly reactive. Many workers observed that organic matter may disperse or agglomerate engineered nanomaterials in aqueous media depending on their proportions [64-67]. In soil, engineered nanomaterials may bind with organic matter and charged clay particles through cation bridging [68]; which could gradually introduce the nano-form metallic nutrients (in this case Fe) to the cation exchange sites of the soil and transform them into easily exchangeable forms.

The greater surface area owing to smaller size of OCIO resulted in significant reduction in hydrodynamic diameter of the nanomaterial treated soil samples; which in turn probably influenced the bioavailability of the nutrient elements. Overall, a strong positive correlation among the release patterns of Fe, N, and P in various soil and aqueous conditions was evidenced in this study. Interestingly, the ζ-potential of the soil was negative prior spiking with OCIO; while, after spiking the ζ-potential became positive. In fact the ζ-potential of soil was more positive under low dose application of nanomaterials. This indicated that the cation holding capacity of the soil remarkably increased in presence of nanomaterials in smaller amount [28]. Moreover, the hydrodynamic diameters of soil particles were smaller when nanomaterials were spiked in smaller amount (10 mg kg^{-1}) than larger quantity (50 mg kg^{-1}). Occurrence of nanomaterials in high concentration in media increases homo-aggregation through greater collision and reduction in particle repulsive force [28,42]. Presumably, the slow release profile attributed by the capping agent might balance the dispersion-agglomeration dynamics of the nanomaterials.

5.5.5. Performance of OCIO as a soil conditioner in Fe rich and deficient arable soil

OCIO were introduced to soil-plant system in step-by-step manner. At first, they were applied to soil samples devoid of plants in laboratory; then, they were incorporated in tomato grown artificially leached and natural soil. Surprisingly, in all situations, Fe release profile followed exactly similar pattern. The pH of the originally acidic soil shifted towards neutral range; and NPK-availability uniformly increased in all conditions. We also observed spectacular improvement in other soil health parameters (SOC, BD, WHC, nitrogen and activity of urease and phosphatase enzyme). This may be due to the oxalate capping on synthesized materials; because such coatings can be used as energy source by the soil micro-organisms and the dissociated oxalates in soil system enhance C stock [9,69,70]. Moreover, the nano-structure of our material might have enhanced the soil porosity thereby improved the water retention capacity [9].

In general, pH change towards “point zero charge” (neutrality), induce agglomeration of nanoparticles due to reduction in electrostatic repulsive forces between particles [42]. As such, increase in agglomeration leads to enhanced water retention in soil through enlargement of soil pores [71]. Here, the reduction in BD

indicates increment in voids in the soil (Table 5.15). Therefore, the increment in pH probably induced dispersion of the oxalate capped OCIO in soil, which in turn, increased water retention capacity of the soil through enhancement of pore spaces.

Iron oxide nanoparticles being highly reactive in soil readily release Fe^{2+} or Fe^{3+} ions [72,73]. Such release could greatly restore the C levels in soil through formation of soluble complexes with the soil organic matter molecules [74]. Iron is also an important co-factor for several soil enzymes [5]. Although iron-based nanoparticles induce toxicity through generation of reactive oxygen species (ROS), chemically stable Fe_3O_4 have no environmental toxicology [5]. On the other hand, predominance of Fe^{2+} in soil solution generally leads to acceleration in NO_3 reduction through activation of N reducing bacteria (*Bacillus sp.*) which may induce denitrication loss of N in certain conditions [52,75]. Such possibilities are highly obvious when $FeSO_4$ is used as fertilizer. Interestingly, the oxalate capping in our material should reduce the pace of NO_3 reduction in soil because the Fe release from OCIO was significantly slower than $FeSO_4$ which warrants in-depth research in future for improving bio-compatibility of OCIO. Hence, the highly oxidized crystals in our material render greater stability in the soil environment, which in turn, might have induced urease activity.

Previously, Zhou et al. [72] showed reduction in P availability in soil due to incorporation of iron oxide (FeO, Fe_2O_3, and Fe_3O_4) which suppressed the acid phosphatase activity. However, they did not mention the dose dependency of such a phenomenon. In contrast, He et al. [5] proposed that Fe_3O_4 nanoparticles provide beneficial nutrients to soil bacteria which, in turn, greatly stimulate enzyme production in soil. The Fe^{3+} predominance in soil was likely to be higher than Fe^{2+} that is known to generate oxidative stress [76]; and Fe^{3+} and Fe^{2+} were in 2 : 1 ratio in OCIO. Thus, the chance of inhibition in bacterial proliferation was less and application of OCIO at a low dose (10 mg kg^{-1}) was beneficial with respect to P and Fe nutrition in soil.

In nature, Fenton-like system can be established due to presence of oxalic acid, Fe, and sunlight [77]. The use of oxalic acid in the synthesis process ensured the oxalate capping over Fe_2O_3 in our material. Therefore it can be speculated that sunlight exposure of OCIO in agricultural fields should create a photo Fe–oxalate

system which is highly efficient in degrading toxic organic pollutants like pentachlorophenol [77,78]. Interestingly, in this study the OCIO exhibited a slow but steady Fe release profile mainly due to the oxalate capping; which presumably should establish a homogenous photo-Fe–oxalate system where Fe exist in a soluble form [77]. As a result, the photoactivity of the material is not likely to interact with Fe bioavailability in soil. Such multifarious traits of OCIO can enhance the value of the material in practice.

5.5.6 Plant health and productivity

Song et al. [79] reported elevated activity of reactive oxygen species (ROS) scavenging enzymes (Peroxidase, Catalase, and SOD) in *Lemna minor* due to CuONP exposure. Several other workers also reported adverse impacts of CuONPs on fish, crustaceans, and soil bacteria [80-82]. In contrast, we evidenced significantly low catalase and SOD activity in OCIO treated plants than those treated with $FeSO_4$ and Fe-EDTA. Predominance of free radicals removes electron from the lipids in the cell membrane and leads to cell damage [83]. However, the OCIO did not induce oxidative stress in tomato because lipid peroxidation was significantly low in nano-exposed plants.

In general, engineered Fe, Mn, Cu, and Zn-nanoparticles were non-toxic in low concentration to lettuce, and significantly augmented plant growth [84]. However, these studies are conducted in soil-less media or in controlled laboratory condition. In this context, we recorded prolific growth and yield of tomato due to soil application of OCIO; we observed magnificent enhancement in germination rate, root and shoot elongation of *V. radiata and V. mungo* in aqueous media contributed by OCIO compared to $FeSO_4$, Fe-EDTA, and Fe-oxalate.

When OCIO was applied in large scale in field for catering the growth and development of tomato; the lowest dose of OCIO (OCIO 2 kg ha^{-1}) significantly augmented nutrient (Fe, N, and P) uptake. However, the uptake of Fe was lower in $FeSO_4$ treated plants that OCIO treated ones, whereas the overall Fe availability was greater in $FeSO_4$ treated plots. Interestingly, such results were more conspicuous in the second year as compared to the first year of cultivation. This approved that the OCIO has had a long term conditioning impact on overall quality of the soil and the greater efficiency of the nano form of iron cannot be overruled. Overall, OCIO incorporation in field soil resulted in greater yield potential with longer and better

storage quality of the produce as compared to the conventionally grown tomato. Moreover, the lycopene contents of the OCIO (2 kg ha^{-1}) fruits were also remarkable. Lycopene renders the red color to the tomato fruits and thus has immense importance in regard to the marketability of the produce [85]. Lycopene content is also a good indicator of the suitability of the growing condition [86]. In general, lycopene redness (i.e., lycopene contents) of tomato fruits this study, is largely governed by the nutrient balance in soil and their uptake in plants [87]. Therefore, increased bioavailability of all the nutrients due to application of OCIO as soil amendments probably facilitated lycopene production in the fruits.

5.6. Conclusion

A novel and easy large-scale synthesis route for iron oxalate capped iron-oxide (OCIO) nanomaterial was developed avoiding high temperature calcination. The material was synthesized with a specific goal to utilize it as a soil conditioner that renders optimum iron nutrition to plants in varied kind of soil reaction and fertility status. The OCIO material did not show any inhibitory effects on beneficial soil bacteria (NFBs and PSBs). Moreover, profuse germination of OCIO treated black gram and green gram seeds not only confirmed the ecofriendly property of OCIO but also showed high promise of the material as a prolific plant growth promoter. Whereas, seed germination greatly retarded due to exposure of $FeSO_4$, Fe-EDTA, and Fe-oxalate exposure. The research presented here demonstrates the excellence of OCIO in regard to soil quality restoration and plant development. Fascinatingly, the material recovered iron and phosphorous availability in a nutrient-starved soil and sustained plant growth potential. OCIO possesses a unique H^+ scavenging property which facilitates to rectify aberrant pH thereby assuring a steady iron release. This quality also indirectly helps to sustain phosphorous solubility in soil. 10 and 20 mg kg^{-1} of OCIO significantly improved soil health (N, P, organic C status, and urease and phosphatase activity) as compared to Fe–EDTA and $FeSO_4$ in pot culture experiment. All such benefits were duly extrapolated in tomato cultivated soil; and, the 2 kg ha^{-1} was found to be the most effective dose for alluvial soil (inceptisols). However, high efficiency and low toxicity was achieved when we applied the OCIO in low concentration. The OCIO treated plants showed least activity of oxidative inducible enzymes and poor lipid peroxidation; which are definite indicators of abiotic stress in

plant species. In summary, this research showcased novel synthesis and unique agricultural potentiality of iron (oxalate) capped Fe-oxide nanomaterials, substantiated by scientific understandings.

Bibliography

[1] Robinson, N. J., Procter, C. M., Connolly E. L., and Guerinot, M. L. A ferric-chelate reductase for iron uptake from soils. *Nature*, 397:694–697, 1999.

[2] Tavakoli, M. T., Chenari, A. I., Rezaie, M., Tavakoli, A., Shahsavari, M., and Mousavi, S. R. The Importance of Micronutrients in Agricultural Production. *Advances in Environmental Biology*, 8(10):31-35, 2014.

[3] Chen, Y. and Barak, P. Iron Nutrition of plants in calcareous soils. *Advances in agronomy*, 35:217-240, 1982.

[4] Sillanppa, M. *Trace Elements in Soils and Agriculture*. Food & Agriculture Organization of the United Nations, Rome, Issue 17, 1972.

[5] He, S., Feng, Y., Ren, H., Zhang, Y., Gu, N., and Lin, X. The Impact of Iron Oxide Magnetic Nanoparticles on the Soil Bacterial Community. *Journal of Soils and Sediments*, 11:1408–1417, 2011.

[6] Sheykhbaglou, R., Sedghi, M., Tajbakhsh shishevan, M., and Sharifi, S. R. Effects of nano-iron oxide particles on agronomic traits of soybean. *Notulae Scientia Biologicae*, 2:112–113, 2010.

[7] Carabante, I., Grahn, M., Holmgren, A., Kumpiene, J., and Hedlund, J. Adsorption of As (V) on iron oxide nanoparticle films studied by in situ ATR-FTIR spectroscopy. *Colloids and Surfaces A-Physicochemical and Engineering Aspects*, 346:106–113, 2009.

[8] Liu, G., Mylavarapu, R., Hanlon, E., and Lee, C. Soil pH management for optimum commercial fruit production in florida. *Horticultural Sciences*, 4:1–6, 2014.

[9] Das, P., Sarmah, K., Hussain, N., Pratihar, S., Das, S., Bhattacharyya, P., Patil, S. A., Kim, H. S., Khazi, M. I. A., and Bhattacharya, S. S. Novel Synthesis of an Iron Oxalate Capped Iron Oxide Nanomaterial: A Unique Soil Conditioner and Slow Release Eco-Friendly Source of Iron Sustenance in Plants. *RSC Adv*ances, 6:103012–103025, 2016.

[10] CLSI. Performance Standards for Antimicrobial Disk Susceptibility Testing; Twenty-Second Informational supplement. CLSI document M100-S22, Clinical and Laboratory Standards Institute, Wayne, 2012.

[11] Pramer, D. and Schmidt, E. L. *Experimental Soil Microbiology*. Burgess Publication, Minneapolis, 1964.

[12] Karak, T., Paul, R. K., Sonar, I., Sanyal , S., Ahmed, K. Z., Boruah , R. K., Das, D. K., and Dutta, A. K. Chromium in soil and tea (*Camellia sinensis L.*) infusion: Does soil amendment with municipal solid waste compost make sense? *Food Research International*, 64:114–124, 2014.

[13] El-Temsah, Y. S. and Joner, E. J. Impact of Fe and Ag Nanoparticles on Seed Germination and Differences in Bioavailability during Exposure in Aqueous Suspension and Soil. *Environmental Toxicology*, 27:42–49, 2012.

[14] Abei, H., Wyss, S. R., Scherz, B., and Skvaril, F. Heterogeneity of erythrocyte catalase II. Isolation and characterization of normal and variant erythrocyte catalase and their subunits. *European Journal of Biochemistry*, 48:137–145, 1974.

[15] Ellman, G. L. Tissue sulphydryl groups. *Archives of Biochemistry*, 82:70–77, 1959.

[16] Martin, J. P. J., Dailey, M., and Sugarman, E. Negative and Positive Assays of Superoxide Dismutase Based on Hematoxylin Autoxidation. *Archives of Biochemistry and Biophysics*, 255:329–336, 1987.

[17] Dhindsa, R. S., Plumb-Dhindsa, P., and Thorpe, T. A. Leaf Senescence: Correlated with Increased Levels of Membrane Permeability and Lipid Peroxidation, and Decreased Levels of Superoxide Dismutase and Catalase. *Journal of Experimental Botany*, 32:93–101, 1981.

[18] Lowry, O. H., Rosebrough, N. J., Farr, A. L., and Randall, R. J. Protein measurement with the folin phenol reagent. *Journal of Biological Chemistry*, 193:265–275, 1951.

[19] Page, A. L., Miller, R. H., and Keeney, D. R. *Methods of Soil Analysis*. Part 2. Soil Science Society of America, Madison, Wisconsin, USA, 1982.

[20] APHA, *Standard methods for the examination of water and wastewater*. American Public Health Association, Washington DC, 20th edition, 1999.

[21] Tandon, H. L. S. *Methods of analysis of soils, plants, waters and fertilizers*. Fertilizer Development and Consultation Organization, New Delhi, 1995.

[22] Tabatabai, M. A. and Bremner, J. M. Use of p-nitrophenol phosphate for the assay of soil phosphatase activity. *Soil Biology and Biochemistry*, 1:301–307, 1969.

[23] Ignat, T., Schmilovitch, Z., Fefoldi, J., Bernstein, N., Steiner, B., Egozi, H., and Hoffman, A. Nonlinear methods for estimation of maturity stage, total chlorophyll, and carotenoid content in intact bell peppers. *Biosystems Engineering*, 114 (4):414–425, 2013.

[24] Subbiah, B. V. and Asija, G. L. A Rapid Procedure for Estimation of Available Nitrogen in Soil. *Current Science*, 25 (8):259-260, 1956.

[25] Tabatabai, M. A. and Bremner, J. M. Assay of urease activity in soils. *Soil Science Society of America*, 41:350–352, 1972.

[26] Vance, E. D., Brookes, P. C., and Jenkinson, D. S. An extraction method for measuring soil microbial biomass C. *Soil Biology and Biochemistry*, 19:703–707, 1987.

[27] Lindsay, W. L. and Norvell, W. A. Development of a DTPA Soil Test for Zinc, Iron, Manganese, and Copper1. *Soil Science Society of America Journal*, 42:421–428, 1978.

[28] Das, P., Barua, S., Sarkar, S., Chatterjee, S. K., Mukherjee, S., Goswami, L., Das, S., Bhattacharya, S., Karak, N., and Bhattacharya, S. S. Mechanism of Toxicity and Transformation of Silver Nanoparticles: Inclusive Assessment in Earthworm-Microbe-Soil-Plant System. *Geoderma*, 314:73–84, 2018.

[29] Lugasi, A., Biro, L., Hovarie, J., Sagi, K.V., Brandt, S., and Barna, E. Lycopene content of foods and lycopene intake in two groups of the Hungarian population. *Nutrition Research*, 23:1035-1044, 2003.

[30] Vishniac, W. Methods for study of the Hill reaction. In Colowick, S. P., Kaplan, N.O. editors, *Methods Enzymol*, pages 342–343, Academic Press, New York, 1957.

[31] Kwinta, J. and Cal, K. Effects of salinity stress on the activity of glutamine Synthetase and glutamate dehydrogenase in triticale seedlings. *Polish Journal of Environmental Studies*, 14 (1):125–130, 2005.

[32] Esposito, S., Guerriero, G., Vona, V., Di Martino Rigano, V., Carfagna, S., and Rigano, C. Glutamate Synthase Activities and Protein Changes in Relation to Nitrogen Nutrition in Barley: The Dependence on Different Plastidic Glucose-6P Dehydrogenase Isoforms. *Journal of Experimental Botany*, 56:55–64, 2005.

[33] Radin, J. W. Distribution and development of nitrate reductase activity in germinating cotton seedlings. *Plant Physiology*, 53(3):458–463, 1974.

[34] Chance, B. and Maehly, A. C. Assay of catalases and peroxidases. *Methods in Enzymology*, 2:764–775, 1955.

[35] Pande, S., Jana, S., Basu, A. K., Sinha, A., Dutta, A. and Pal, T. Nanoparticle-Catalyzed Clock Reaction. *The Journal of Physical Chemistry C*, 112 (10):3619-3626, 2008.

[36] Pegu, R., Majumdar, K. J., Talukdar, D. J., and Pratihar, S. Oxalate capped iron nanomaterial: from methylene blue degradation to bis (indolyl) methane synthesis. *RSC Advances*, 4:33446–33456, 2014.

[37] Aragon, M. J., Leon, B., Vicente, C. P., and Tirado, J. L. Synthesis and Electrochemical Reaction with Lithium of Mesoporous Iron Oxalate Nanoribbons. *Inorganic Chemistry*, 47:10366, 2008.

[38] Woo, K., Hong, J., Choi, S., Lee, H. W., Ahn, J. P., Kim, C. S., and Lee, S. W. Easy Synthesis and Magnetic Properties of Iron Oxide Nanoparticles. *Chemistry of Materials*, 16:2814, 2004.

[39] Yamashita, T. and Hayes, P. Analysis of XPS spectra of Fe^{2+} and Fe^{3+} ions in oxide materials. *Applied Surface Science*, 254:2441– 2449, 2008.

[40] Grosvenor, A. P., Kobe, B. A., Biesinger, M. C., and McIntyre, N. S. Investigation of multiple splitting of Fe 2p XPS spectra and bonding in iron compounds. *Surface and Interface Analysis*, 36:1564–1574, 2004.

[41] Conway, J. R., Beaulieu, A. L., Beaulieu, N. L., Mazer, S. J., and Keller, A. A. Environmental Stresses Increase Photosynthetic Disruption by Metal Oxide Nanomaterials in a Soil-Grown Plant. *ACS Nano*, 9:11737–11749, 2015.

[42] Tourinho, P. S., Van Gestel, C. A. M., Lofts, S., Svendsen, C., Soares, A. M. V. M., and Loureiro, S. Metal-Based Nanoparticles in Soil: Fate, Behavior, and Effects on Soil Invertebrates. *Environmental Toxicology and Chemistry*, 31:1679–1692, 2012.

[43] Heckmann, L. H., Hovgaard, M. B., Sutherland, D. S., Autrup, H., Besenbacher, F., and Scott-Fordsmand, J. J. Limit-Test Toxicity Screening of Selected Inorganic Nanoparticles to the Earthworm *Eisenia Fetida*. *Ecotoxicology*, 20:226–233, 2011.

[44] Gomes, S. I. L., Novais, S. C., Scott-Fordsmand, J. J., De Coen, W., Soares, A. M. V. M., and Amorim, M. J. B. Effect of Cu-Nanoparticles versus Cu-Salt in *Enchytraeus Albidus* (Oligochaeta): Differential Gene Expression through

Microarray Analysis. *Comparative Biochemistry and Physiology - Part C: Toxicology & Pharmacology*, 155:219–227, 2012.

[45] Diez-Ortiz, M., Lahive, E., Kille, P., Powell, K., Morgan, A. J., Jurkschat, K., Van Gestel, C. A. M., Mosselmans, J. F. W., Svendsen, C., and Spurgeon, D. J. Uptake Routes and Toxicokinetics of Silver Nanoparticles and Silver Ions in the Earthworm Lumbricus Rubellus. *Environmental Toxicology and Chemistry*, 34:2263–2270, 2015.

[46] Mehta, C. M., Srivastava, R., Arora, S., and Sharma, A. K. Impact assessment of silver nanoparticles on plant growth and soil bacterial diversity. *3 Biotech*, 6: 254, 2016.

[47] Bartakova, I., Kummerova, M., Mandl, M., and Pospisil, M. Phytotoxicity of iron in relation to its solubility conditions and the effect of ionic strength. *Plant and Soil*, 235:45–51, 2001.

[48] Liba, C. M., Ferrara, F. I. S., Manfio, G. P., Fantinatti-Garboggini, F., Albuquerque, R. C., Pavan, C., Ramos, P. L., Moreira-Filho, C. A, and Barbosa, H. R. Nitrogen-fixing chemo-organotrophic bacteria isolated from cyanobacteria-deprived lichens and their ability to solubilize phosphate and to release amino acids and phytohormones. *Journal of Applied Microbiology*, 101(5):1076–1086, 2006

[49] Hameeda, B., Harini, G., Rupela, O. P., Wani, S. P., and Reddy, G. Growth promotion of maize by phosphate solubilizing bacteria isolated from composts and macro fauna. *Microbiological Research*, 163 (2):234–242, 2008.

[50] Hussain, N., Singh, A., Saha, S., Satish Kumar, M. V., Bhattacharyya P., and Bhattacharya, S. S. Excellent N-fixing and P-solubilizing traits in earthworm gut-isolated bacteria: A vermicompost based assessment with vegetable market waste and rice straw feed mixtures. *Bioresource Technology*, 222:165–174, 2016.

[51] Rodriguez-Rojo, S., Visentin, A., Maestri D., and Cocero, M. J. Assisted extraction of rosemary antioxidants with green solvents. *Journal of Food Engineering*, 109:98–103, 2012.

[52] Liu, T., Li, X., Zhang, W., Hu, M., and Li, F. Fe(III) Oxides Accelerate Microbial Nitrate Reduction and Electricity Generation by *Klebsiella Pneumoniae* L17. *Journal of Colloid and Interface Science*, 423:25–32, 2014.

[53] Waychunas, G. A., Kim, C. S., and Banfield, J. F. Nanoparticulate Iron Oxide Minerals in Soils and Sediments: Unique Properties and Contaminant Scavenging Mechanisms. *Journal of Nanoparticle Research*, 7:409–433, 2005.

[54] Chen, K. L. and Elimelech, M. Aggregation and deposition kinetics of fullerene (C60) nanoparticles. *Langmuir*, 22 (26):10994–11001, 2006.

[55] El Badawy, A. M., Luxton, T. P., Silva, R. G., Scheckel, K. G., Suidan, M. T., and Tolaymat, T. M. Impact of environmental conditions (pH, ionic strength, and electrolyte type) on the surface charge and aggregation of silver nanoparticles suspensions. *Environmental Science & Technology*, 44:1260–1266, 2010.

[56] Reddy, T.Y., and Reddi, G. H. S. *Principles of Agronomy*. Kalyani Publishers, Noida, India, 1992.

[57] Stumm, W. and Morgan, J. J. *Aquatic Chemistry*. Wiley-VCH Verlag GmbH, 3rd edition, 1996.

[58] Avramescu, M. L., Rasmussen, P. E., Chenier, M., and Gardner, H. D. Influence of pH, Particle Size and Crystal Form on Dissolution Behaviour of Engineered Nanomaterials. *Environmental Science and Pollution Research International*, 24:1553–1564, 2017.

[59] Shih, C. J., Lin, S., Sharma, R., Strano, M. S., and Blankschtein, D. Understanding the pH-Dependent Behavior of Graphene Oxide Aqueous Solutions: A Comparative Experimental and Molecular Dynamics Simulation Study. *Langmuir*, 28:235–241, 2012.

[60] Goswami, L., Raul, P., Sahariah, B., Bhattacharyya, P., and Bhattacharya, S. S. Characterization and risk evaluation of tea industry coal ash for environmental suitability. *Clean-Soil, Air, Water*, 42(10):1470–1476, 2014.

[61] Bhattacharyya, P., Reddy, K. J., and Attili, V. Solubility and fractionation of different metals in fly ash of Powder River basin coal. *Water Air and Soil Pollution*, 220:327-337, 2011.

[62] Reddy, K. J., Gloss, S. P., and Wang, L. Reaction of CO_2 with alkaline solid wastes to reduce contaminant mobility. *Water Research*, 28:1377-1382, 1994.

[63] Lindsay, W. L. *Chemical Equilibria in Soils*. Wiley-Interscience Publication, Wiley, 1979.

[64] Baalousha, M., Manciulea, A., Cumberland, S., Kendall, K., and Lead, J. R. Aggregation and Surface Properties of Iron Oxide Nanoparticles: Influence of

pH and Natural Organic Matter. *Environmental Science & Technology*, 27:1875–1882, 2008.

[65] Keller, A. A., Wang, H., Zhou, D., Lenihan, H. S., Cherr, G., Cardinale, B. J., Miller, R., and Ji, Z. Stability and Aggregation of Metal Oxide Nanoparticles in Natural Aqueous Matrices. *Environmental Science & Technology*, 44:1962–1967, 2010.

[66] King, S. M. and Jarvie, H. P. Exploring How Organic Matter Controls Structural Transformations in Natural Aquatic Nanocolloidal Dispersions. *Environmental Science & Technology,* 46:6959–6967, 2012.

[67] Goswami, L., Pratihar, S., Dasgupta, S., Bhattacharyya, P., Mudoi, P., Bora, J., Bhattacharya, S. S., and Kim, K. H. Exploring Metal Detoxification and Accumulation Potential during Vermicomposting of Tea Factory Coal Ash: Sequential Extraction and Fluorescence Probe Analysis. *Scientific Reports,* 6:30402, 2016.

[68] Chowdhury, I., Cwiertny, D. M., and Walker, S. L. Combined Factors Influencing the Aggregation and Deposition of Nano-TiO_2 in the Presence of Humic Acid and Bacteria. *Environmental Science & Technology,* 46:6968–6976, 2012.

[69] Tate, R. L. *Soil Microbiology*. John Wiley, 2nd edition, 2000.

[70] Contreras-Ramos, S. M., Alvarez-Bernal, D., and Dendooven, L. Removal of Polycyclic Aromatic Hydrocarbons from Soil Amended with Biosolid or Vermicompost in the Presence of Earthworms (*Eisenia Fetida*). *Soil Biology and Biochemistry*, 40:1954–1959, 2008.

[71] Taha, M. R. and Taha, O. M. E. Influence of nano-material on the expansive and shrinkage soil behavior. *Journal of Nanoparticle Research*, 14 (10):1190, 2012.

[72] Zhou, D. M., Jin, S. Y., Wang, Y. J., Wang, P., Weng N. Y., and Wang, Y. Assessing the Impact of Iron-based Nanoparticles on pH, Dissolved Organic Carbon, and Nutrient Availability in Soils. *Soil and Sediment Contamination*, 21:101–114, 2012.

[73] Waite, T. D., Rose, A. L., Garg, S., and Fujii, M. Superoxide-mediated reduction of ferric iron in natural aquatic systems. *Geochimica et Cosmochimica Acta*, 70 (18):A681, 2006.

[74] Jansen, B., Nierop, K. G. J., and Verstraten, J. M. Influence of pH and metal/carbon ratios on soluble organic complexation of Fe(II), Fe(III) and Al(III) in soil solutions determined by diffusive gradients in thin films. *Analytica Chimica Acta*, 454:259-270, 2002.

[75] Zhang, W., Li, X., Liu, T., and Li, F. Enhanced nitrate reduction and current generation by *Bacillus sp.* in the presence of iron oxides. *Journal of Soils and Sediments*, 12:354–365, 2012.

[76] Auffan, M., Achouak, W., Rose, J., Roncato, M. A., Chaneac, C., Waite, D. T., Masion, A., Woicik, J. C., Wiesner, M. R., and Bottero, J. Y. Relation between the redox state of iron-based nanoparticles and their cytotoxicity toward *Escherichia coli*. *Environmental Science & Technology*, 42:6730–6735, 2008.

[77] Lan, Q., Li, F., Sun, C., Liu, C., and Li, X. Heterogeneous photodegradation of pentachlorophenol and iron cycling with goethite, hematite and oxalate under UVA illumination. *Journal of Hazardous Materials*, 174:64–70, 2010.

[78] Lan, Q., Li, F., Liu, C., and Li, X. Z. Heterogeneous photodegradation of pentachlorophenol with maghemite and oxalate under UV illumination. *Environmental Science & Technology*, 42 (21):7918–7923, 2008.

[79] Song, G., Hou, W., Gao, Y., Wang, Y., Lin, L., Zhang, Z., Niu, Q., Ma, R., Mu, L., and Wang, H. Effects of CuO Nanoparticles on *Lemna Minor*. *Botanical Studies*, 57(1):3, 2016.

[80] Zhao, J., Wang, Z., Liu, X., Xie, X., Zhang, K., and Xing, B. Distribution of CuO Nanoparticles in Juvenile Carp (*Cyprinus Carpio*) and Their Potential Toxicity. *Journal of Hazardous Materials*, 197:304-10, 2011.

[81] Li, Y., Zhang, W., Niu, J., and Chen, Y. Mechanism of Photogenerated Reactive Oxygen Species and Correlation with the Antibacterial Properties of Engineered Metal-Oxide Nanoparticles. *ACS Nano,* 6(6):5164-73, 2012.

[82] Collins, D., Luxton, T., Kumar, N., Shah, S., Walker, V. K., and Shah, V. Assessing the Impact of Copper and Zinc Oxide Nanoparticles on Soil: A Field Study. *PLoS One*, 7:e42663, 2012.

[83] Ostrea, E. M. J., Cepeda, E. E., Fleury, C. A., and Balun, J. E. Red Cell Membrane Lipid Peroxidation and Hemolysis Secondary to Phototherapy. *Acta Paediatrica Scandinavica*, 74:378–381, 1985.

[84] Liu, R., Zhang, H., and Lal, R. Effects of Stabilized Nanoparticles of Copper, Zinc, Manganese, and Iron Oxides in Low Concentrations on Lettuce (*Lactuca Sativa*) Seed Germination: Nanotoxicants or Nanonutrients? *Water, Air, & Soil Pollution*, 227:42, 2016.

[85] Nguyen, M. L. and Schwartz, S. J. Lycopene: chemical and biological properties. *Food Technology*, 53:2, 1999.

[86] Sahlin, E., Savage, G. P., and Lister, C. E. Investigation of the antioxidant properties of tomatoes after processing. *Journal of Food Composition and Analysis*, 17:635–647, 2004.

[87] Avila-Juarez, L. A., Gonzalez, R. N., Pina, R., Guevara González, R. G., Torres Pacheco, I., Ocampo Velázquez, R.V., and Moustapha, B. Vermicompost leachate as a supplement to increase tomato fruit quality. *Journal of Soil Science and Plant Nutrition*, 15 (1):46-59, 2015.